Caustics as the Natural Boundaries of the Simulated Dark Matter Web

Sergei Shandarin

Introduction

Zeldovich Approximation (1970)

1 Gravitational Instability

1.1 The Transformation Excluding the Expansion of the Universe

Comoving coordinates, $\mathbf{x}$, and peculiar velocities, $\mathbf{v}_p$, are defined

$$\mathbf{x} = \frac{1}{a(t)}\mathbf{r}, \tag{1}$$

$$\mathbf{v}_p = \mathbf{v} - H(t)\mathbf{r} = a(t)\frac{d\mathbf{x}}{dt}, \tag{2}$$

where $a(t) = (1+z)^{-1}$ is the scale factor, assuming the normalization: $a(present\ time) = 1$; $H(t) = \dot{a}/a$ is the Habble parameter $(H(present\ time) = H_0 = 100\,h\ km\,s^{-1}\,Mpc^{-1})$.

Assuming the $\Lambda = 0$ universe and $p = 0$, the density $\rho(\mathbf{x}, t)$, peculiar velocities $\mathbf{v}_p(\mathbf{x}, t)$, and the perturbation of the gravitational potential $\phi(\mathbf{x}, t)$ are coupled by three nonrelativistic equations

$$\frac{\partial \rho}{\partial t} + \frac{1}{a}\nabla \cdot (\rho \mathbf{v}_p) = -3H\rho, \tag{3}$$

$$\frac{\partial \mathbf{v}_p}{\partial t} + \frac{1}{a}(\mathbf{v}_p \cdot \nabla)\mathbf{v}_p = -\frac{1}{a}\nabla\phi - H\mathbf{v}_p, \tag{4}$$

$$\frac{1}{a^2}\nabla^2\phi = 4\pi G(\rho - \bar{\rho}), \tag{5}$$

where $\bar{\rho} = \bar{\rho}(t)$ is the mean density.

Changing the variable from t to $D \equiv D_g(t)$ and rescaling the density, peculiar velocity and perturbation of the gravitational potential

$$\eta = a^3 \rho, \tag{6}$$

$$\mathbf{v} = (a\dot{D})^{-1}\mathbf{v}_p = \dot{D}^{-1}\frac{d\mathbf{x}}{dt} = \frac{d\mathbf{x}}{dD}, \tag{7}$$

$$\varphi = (\frac{3}{2}\Omega_0 \dot{a}^2 D)^{-1}\phi. \tag{8}$$

one easily obtains

$$\frac{\partial \eta}{\partial D} + \frac{\partial(\eta v_i)}{\partial x_i} = 0, \tag{9}$$

$$\frac{\partial v_i}{\partial D} + v_k \frac{\partial v_i}{\partial x_k} = -\frac{3}{2}\frac{\Omega_0}{D f^2}(\frac{\partial \varphi}{\partial x_i} + v_i), \tag{10}$$

$$\frac{\partial^2 \varphi}{\partial x_i^2} = \frac{\delta}{D}, \tag{11}$$

where $f(t) = d\ln D/d\ln a$, $\delta = (\eta - \bar{\eta})/\bar{\eta} = (\rho - \bar{\rho})/\bar{\rho}$ and summation over dummy indices is assumed.

1.2 Zel'dovich Approximation

Assuming that the linear relation $\partial\varphi/\partial x_i = -v_i$ approximately holds in the nonlinear regime one obtains the set of equations

$$\frac{\partial \eta}{\partial D} + \frac{\partial(\eta v_i)}{\partial x_i} = 0, \tag{12}$$

$$\frac{\partial v_i}{\partial D} + v_k \frac{\partial v_i}{\partial x_k} = 0, \tag{13}$$

$$\frac{\partial^2 \varphi}{\partial x_i^2} = \frac{\delta}{D}. \tag{14}$$

Equation 13 has an obvious solution

$$\mathbf{x}(\mathbf{q}, D) = \mathbf{q} + D\mathbf{v}_0(\mathbf{q}), \tag{15}$$

where $\mathbf{v}_0(\mathbf{q})$ is the initial velocity field. The velocity field remains constant in the Lagrangian space

$$\mathbf{v}(\mathbf{q}, D) = \mathbf{v}_0(\mathbf{q}), \tag{16}$$

but obviously changes with time in the Eulerian space.

Zel'dovich derived the density from the conservation of mass

$$\eta(\mathbf{x}, D)\, d^3x = \bar{\eta}\, d^3q \tag{17}$$

and expressed it in terms of the eigen values $\lambda_1(\mathbf{q})$, $\lambda_2(\mathbf{q})$, and $\lambda_3(\mathbf{q})$ of the initial deformation tensor $d_{ij}(\mathbf{q}) = -\partial v_{0i}/\partial q_j = \partial^2\Phi_0/\partial q_i\,\partial q_j$

(2) There are 4 kinds of fluid elements: which experience 0, 1, 2, or 3 collapses

(1) When and where D*lambda_i = 0 den = infinity (caustic)

$$\eta(\mathbf{q}, D) = \frac{\bar{\eta}}{(1 - D\lambda_1)(1 - D\lambda_2)(1 - D\lambda_3)}. \tag{18}$$

(3) In the limit $\mid D\lambda_i \mid \ll 1$ eq.12 gives the density contrast known from the linear theory

$$\delta(\mathbf{q}, D) \approx D\frac{\partial v_{0j}}{\partial q_j} = D\,(\lambda_1 + \lambda_2 + \lambda_3). \tag{19}$$

I showed that the density can be also drived from the Poisson equation (14) (Doroshkevich, Ryabenki & Shandarin 1973)

$$\tilde{\eta}(\mathbf{q}, D) = \frac{\bar{\eta}}{(1 - D\lambda_1)(1 - D\lambda_2)(1 - D\lambda_3)}(1 - D^2 I_2 + 2D^3 I_3), \tag{20}$$

where $I_2 = \lambda_1\lambda_2 + \lambda_1\lambda_3 + \lambda_2\lambda_3$ and $I_3 = \lambda_1\lambda_2\lambda_3$ are the invariants of the deformation tensor.

If the Zel'dovich solution was exact both would give the same result: $\eta = \tilde{\eta}$.

Obviously η only approximatly equal to $\tilde{\eta}$

$$\frac{\tilde{\eta}}{\eta} = 1 - D^2 I_2 + 2D^3 I_3 \tag{21}$$

but the ratio $\tilde{\eta}/\eta$ remains finite even at $\eta \to \infty$ and $\tilde{\eta} \to \infty$.

In particular, ZA is exact before shell crossing in 1D ($\tilde{\eta}/\eta = 1$ because $I_2 = I_3 = 0$).

1.3 Eigen Values and Invariants

The joint probability distribution of an ordered set of eigenvalues $\lambda_1 > \lambda_2 > \lambda_3$, corresponding to a Gaussian field

$$\boxed{P(\lambda_1, \lambda_2, \lambda_3) = \frac{675\sqrt{5}}{8\pi\ \sigma_\delta^6}(\lambda_1 - \lambda_2)(\lambda_1 - \lambda_3)(\lambda_2 - \lambda_3) \exp\left(\frac{-6I_1^2 + 15I_2}{2\sigma_\delta^2}\right),} \tag{22}$$

where $I_1 = \lambda_1 + \lambda_2 + \lambda_3$ and $I_2 = \lambda_1\lambda_2 + \lambda_1\lambda_3 + \lambda_2\lambda_3$ are the invariants of the deformation tensor; the third invariant is $I_3 = \lambda_1\lambda_2\lambda_3$. Some moments of the eigen values are

$$< \lambda_1 >= - < \lambda_3 >= \frac{3}{\sqrt{10\pi}}\ \sigma_\delta \approx 0.53\ \sigma_\delta, \qquad < \lambda_2 >= 0, \tag{23}$$

$$< \lambda_1^2 >=< \lambda_3^2 >= \frac{13}{30}\ \sigma_\delta^2 \approx 0.43\ \sigma_\delta^2, \qquad < \lambda_2^2 >= \frac{2}{15}\ \sigma_\delta^2 \approx 0.13\ \sigma_\delta^2, \tag{24}$$

$$< \lambda_1\lambda_2 >=< \lambda_2\lambda_3 >= \frac{1}{10}\sigma_\delta^2, \qquad < \lambda_1\lambda_3 >= -\frac{1}{5}\ \sigma_\delta^2, \tag{25}$$

$$< \lambda_1\lambda_2\lambda_3 >= 0. \tag{26}$$

The mean values of the invariants are

$$< I_1 >= 0, \qquad < I_2 >= 0, \qquad < I_3 >= 0. \tag{27}$$

Zel'dovich Approximation (1970)

- Generation of the initial conditions for cosmological N-body simulations (first time in Moscow in 1973, first time in US in 1983)

Key features of cosmic web predicted by ZA

- Anisotropic collapse and anisotropic expansion: pancakes/walls (1970), filaments (1982), along with compact clumps and voids

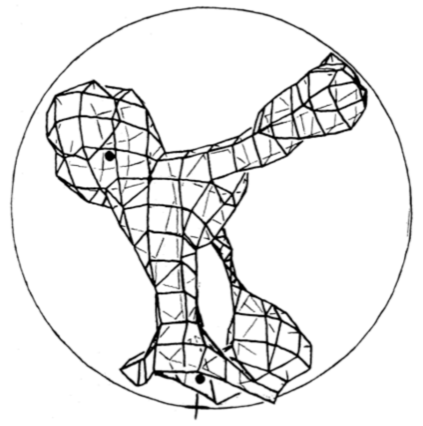

- Full Set of Caustics (1982)

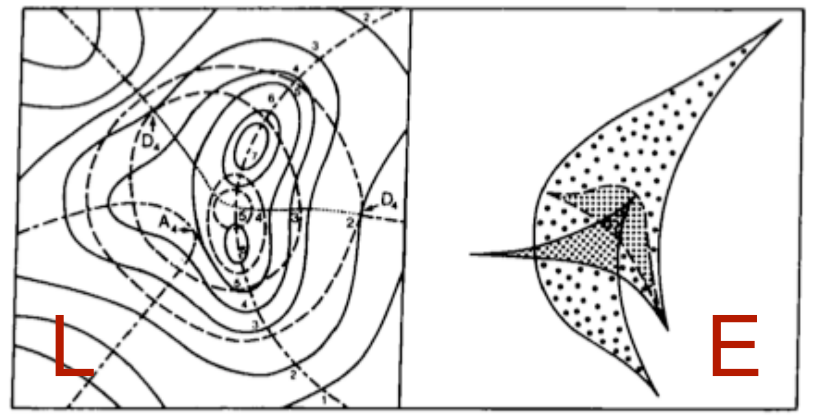

In ZA only
(not in N-body sim.

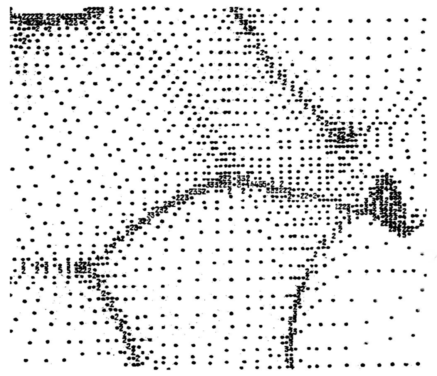

- Connectivity of the Large-Scale structure (1975)

- Topology of LSS (1983)

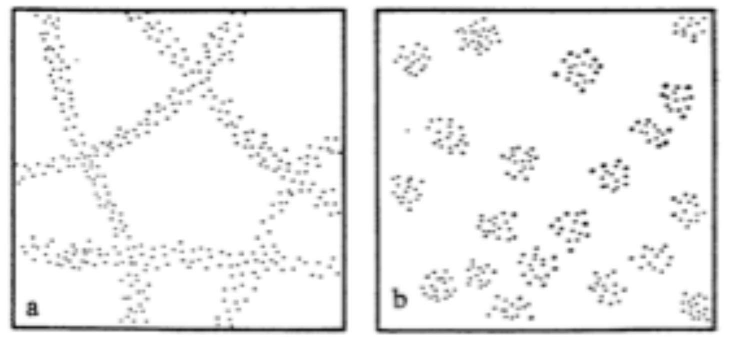

- Multi-stream flows (1970)

- Anisotropic accretion of mass on clumps from filaments (1989)
  https://www.astro.rug.nl/~hidding/go/go.html

Virial theorem

<T>_t is total kinetic energy averaged over time

<V>_t is total potential energy averaged over time

Gravitational potential between two particle ~1/r

results in n=-1

The system must have N_p = const

$$\langle T\rangle_\tau = -\frac{1}{2}\sum_{k=1}^{N}\langle \mathbf{F}_k\cdot\mathbf{r}_k\rangle_\tau = \frac{n}{2}\langle V_{\mathrm{TOT}}\rangle_\tau .$$

First Evidences of Web in Theory and Observations

Zeldovich Approximation
(Z 1970)

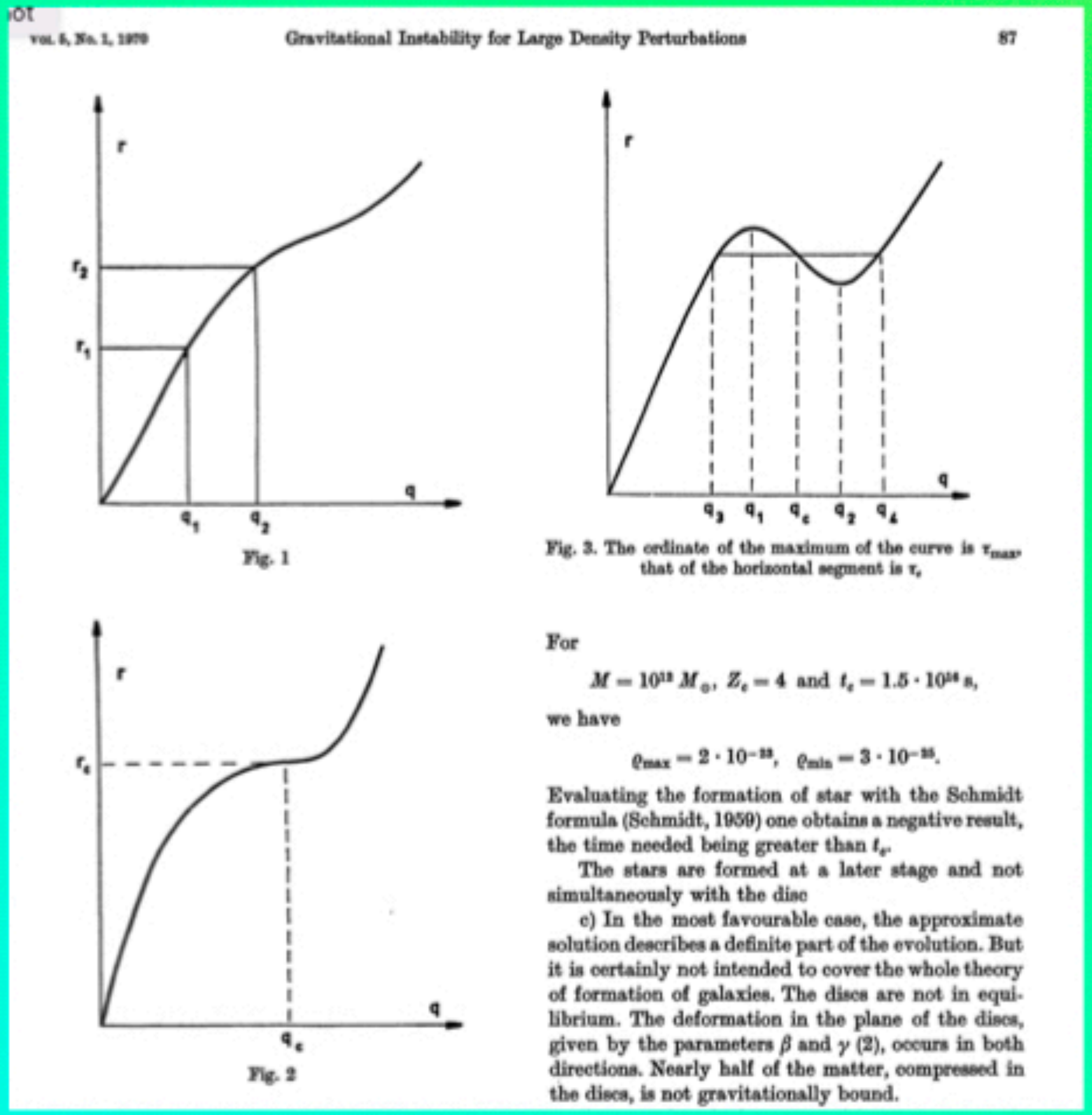
Vol. 5, No. 1, 1970 Gravitational Instability for Large Density Perturbations 87

Fig. 1

Fig. 3. The ordinate of the maximum of the curve is r_{max}, that of the horizontal segment is r_c

Fig. 2

For

$$M = 10^{12} M_{\odot},\ Z_c = 4 \text{ and } t_c = 1.5 \cdot 10^{16}\ \text{s},$$

we have

$$\varrho_{max} = 2 \cdot 10^{-23},\quad \varrho_{min} = 3 \cdot 10^{-25}.$$

Evaluating the formation of star with the Schmidt formula (Schmidt, 1959) one obtains a negative result, the time needed being greater than t_c.

The stars are formed at a later stage and not simultaneously with the disc

c) In the most favourable case, the approximate solution describes a definite part of the evolution. But it is certainly not intended to cover the whole theory of formation of galaxies. The discs are not in equilibrium. The deformation in the plane of the discs, given by the parameters β and γ (2), occurs in both directions. Nearly half of the matter, compressed in the discs, is not gravitationally bound.

25 years later: Hogan **2001**

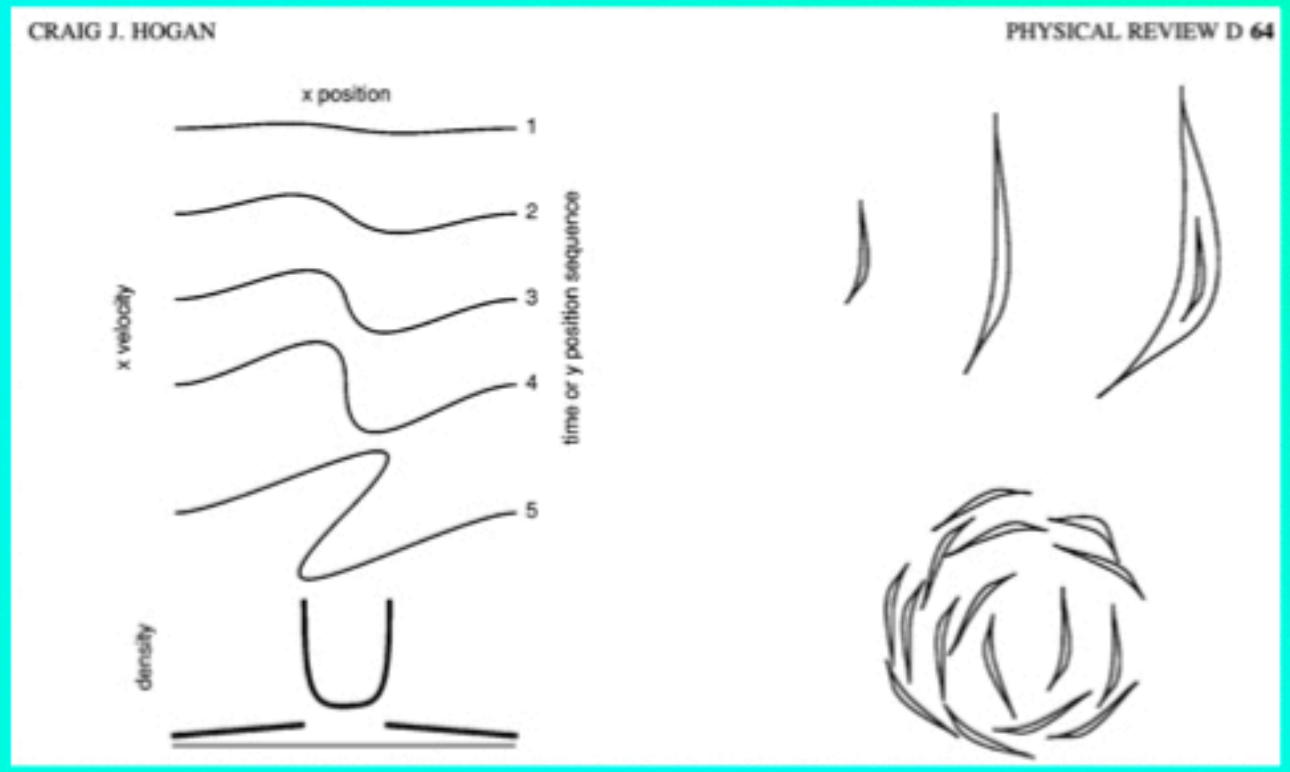

Shandarin 1974

Publications: Doroshkevich, Sunyev, Zeldovich **1975**
Doroshkevich, Shandarin, 1978; Shandarin, Zeldovich 1989
Three or four publications by Einasto)

In DSZ publication the caption state that the plot was made by Shandarin

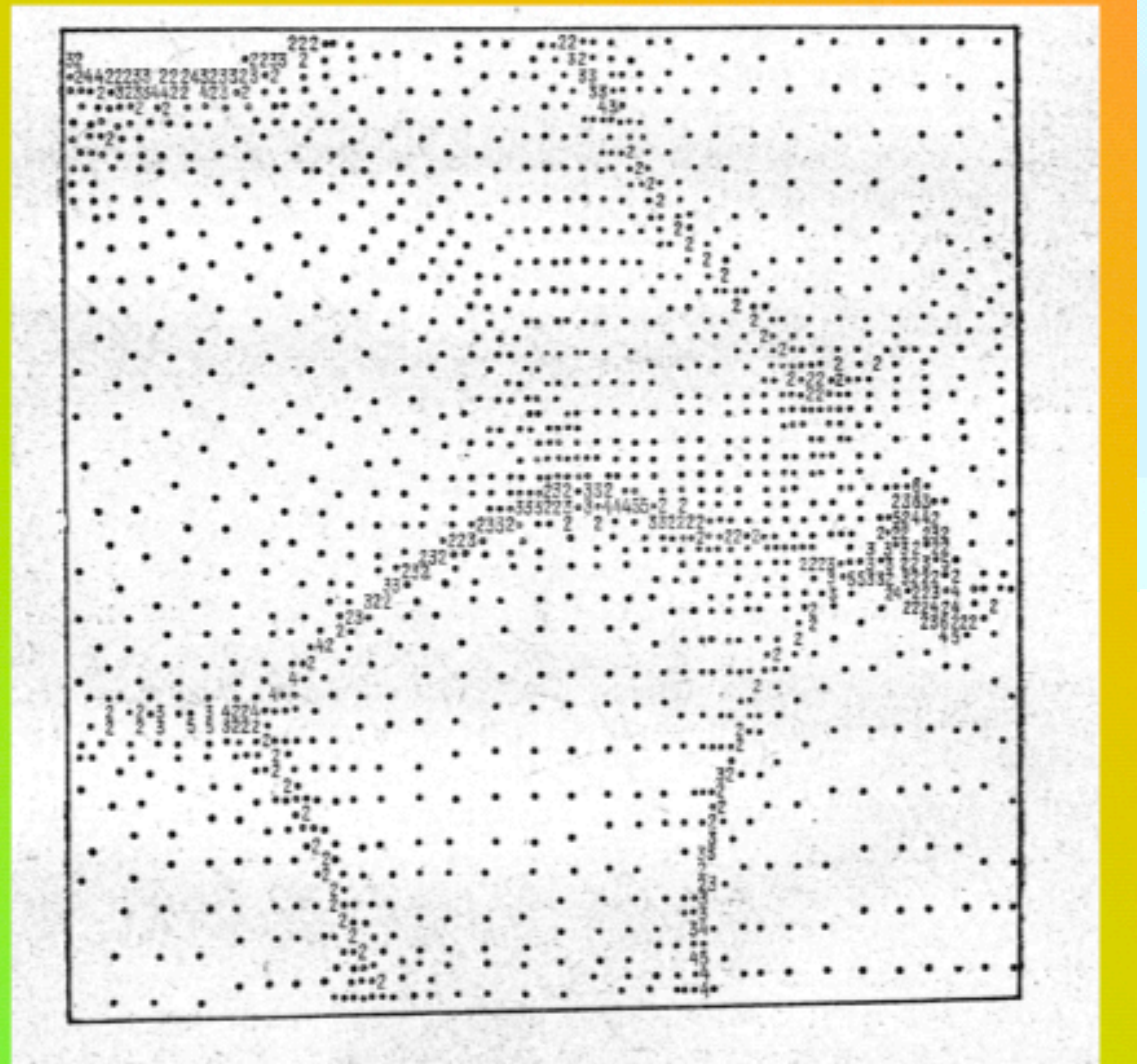

Рис. 15. Типичная картина распределения материальных точек на плоскости, полученная С. Ф. Шандариным при численном моделировании двумерной задачи (см. текст). Числа обозначают число частиц, попавших в одну ячейку. В начале счета частицы располагались в узлах правильной сетки с точностью до малых случайных смещений.

Initial conditions for 3D N-body simulations

Doroshkevich, Rubenkiy, Shandaron **1973**
Translated from Astrofizika, Vol. 9, No. 2, pp. 257-272, April-June, 1973.

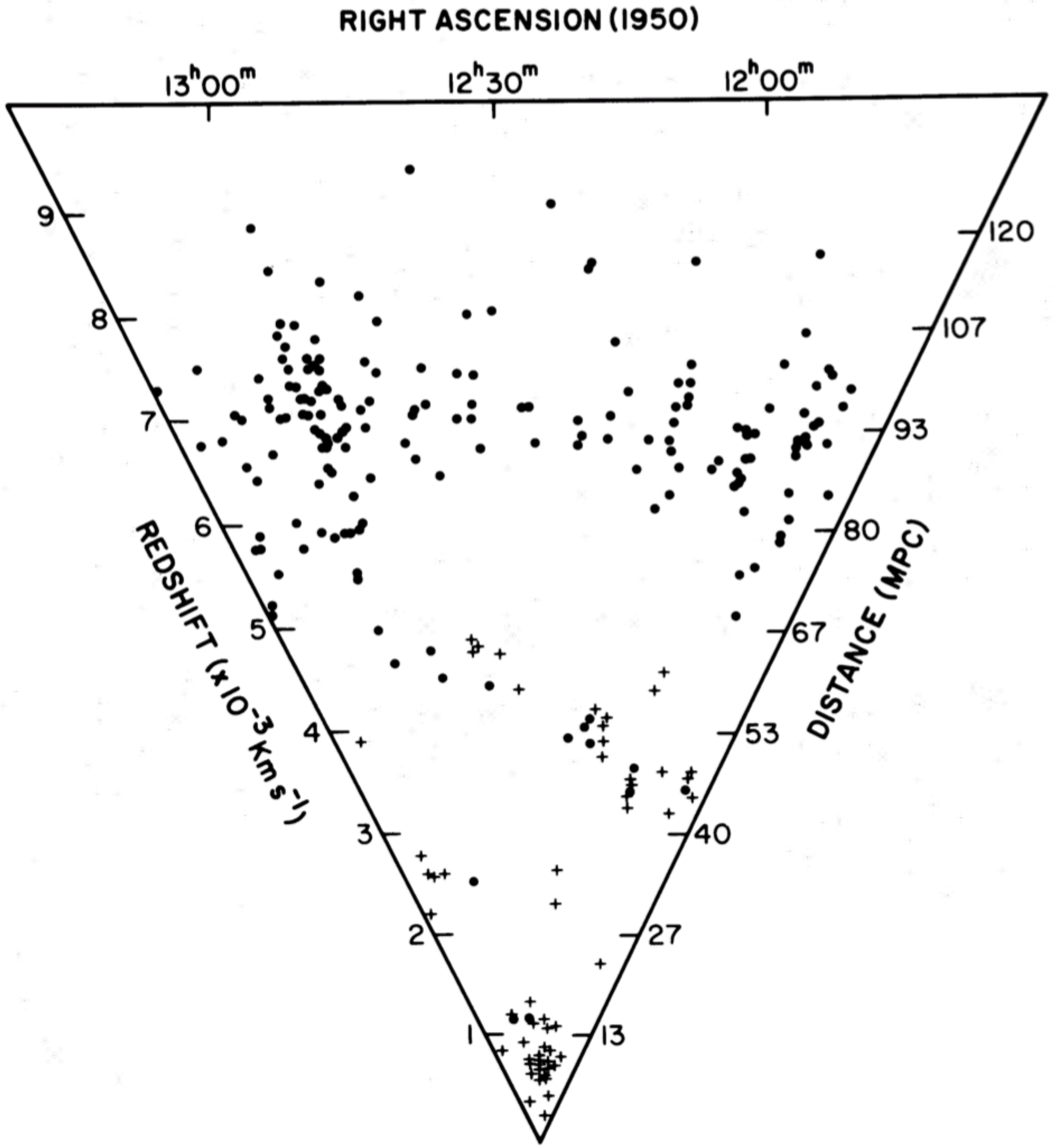

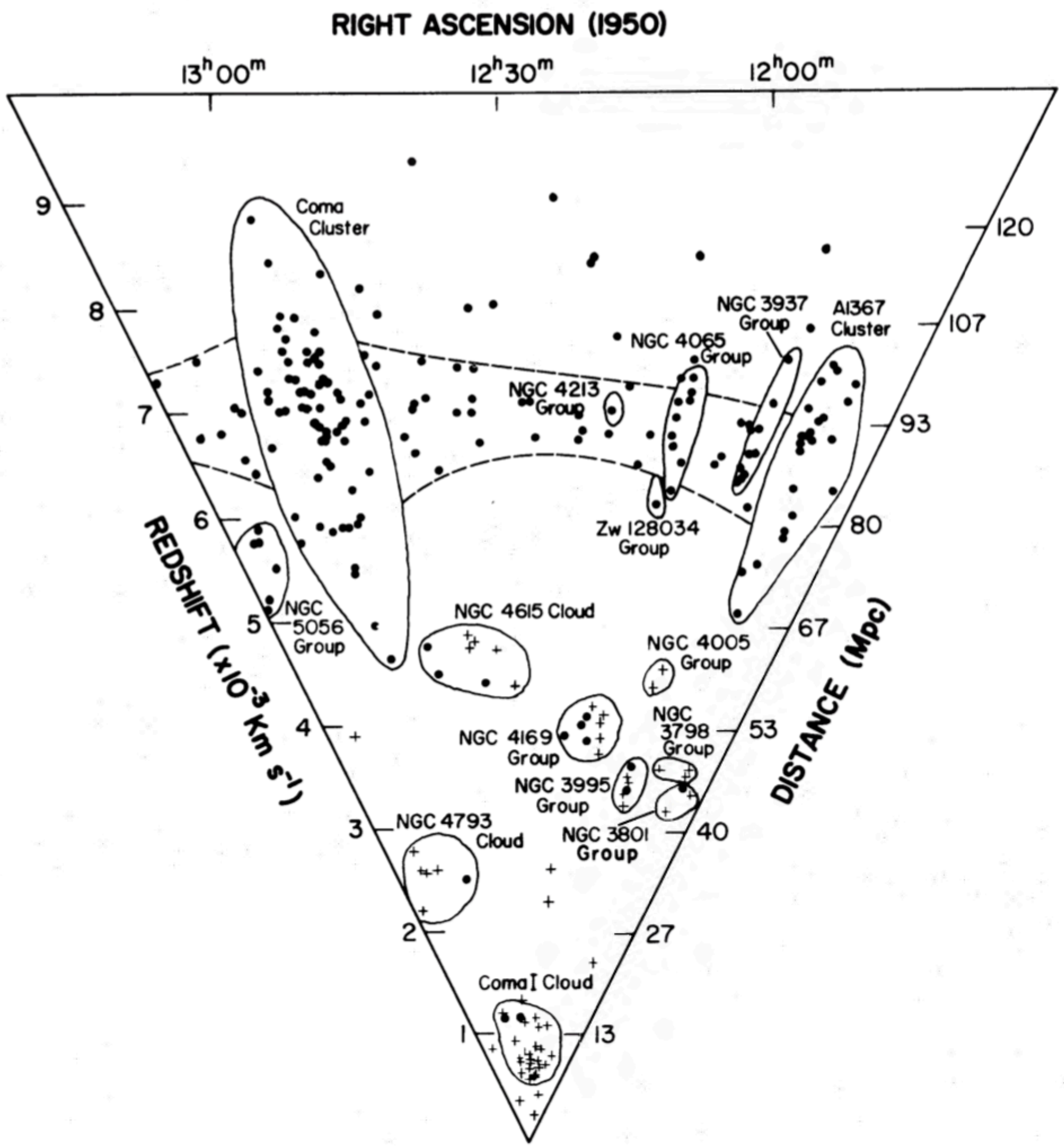

FIG. 2.—(*a*) (*left panel*) Wedge diagram for all galaxies in our sample. The Supercluster is clearly seen at an average redshift of approximately 7000 km s^{-1}. The distribution of foreground galaxies is very clumpy. Those galaxies with $V_0 < 5000$ km s^{-1} that are represented by crosses are too faint to be surveyed if they were at the distance of the Supercluster. The distance scale assumes $H_0 = 75$ km s^{-1} Mpc^{-1}, and the angular size of the survey has been magnified by approximately 2 times. (*b*) (*right panel*) An interpretive form of the wedge diagram.

Gregory, Thompson June 1978

N-body simulations

Shandarin 1981, Erici workshop

In The Origin and Evolution of Galaxies,

Eds. B.J.T. Jones and J.E. Jones

(Reidel, Dordrecht), p.171

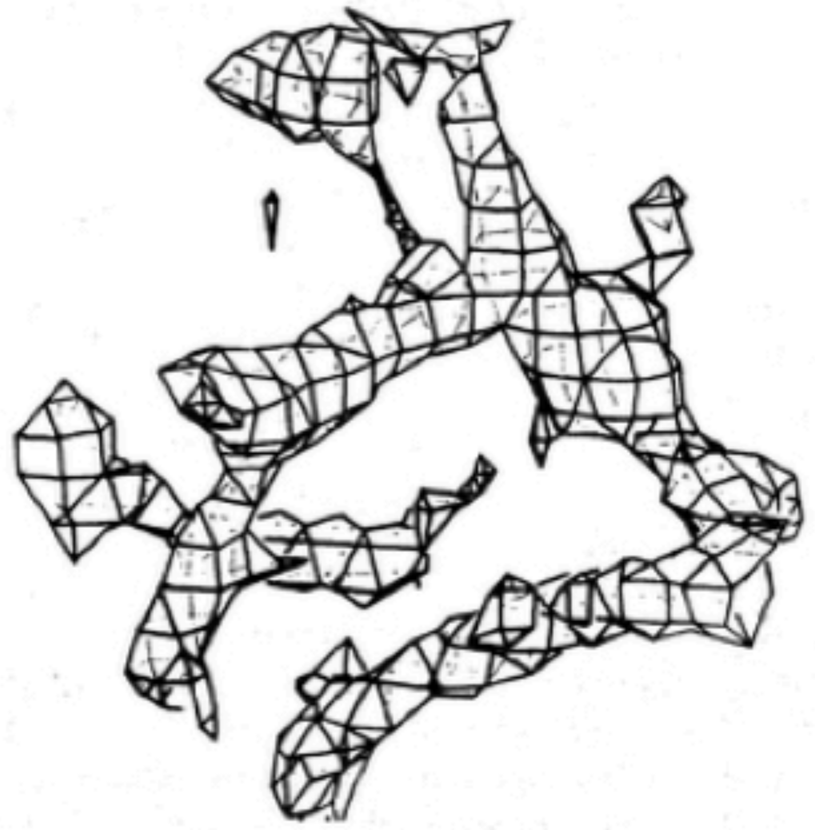

Figure 3. An example of the structures arising in 3D numerical simulations of the adiabatic scenario. The surface is a surface of constant density ρ ~ 2.5 ρ.

Klypin, Shandarin 1983, MNRAS

- **"The region of high density seem to form a single three-dimensional web structure"**

Figure 4. A surface of constant density level is plotted for the same region as that in Fig. 3.

CAUSTICS

(1) Density is formally infinite
(In reality density is discontinuous)

(2) Caustics separate regions with different number of streams

Zeldovich Approximation in 1D

Phase space

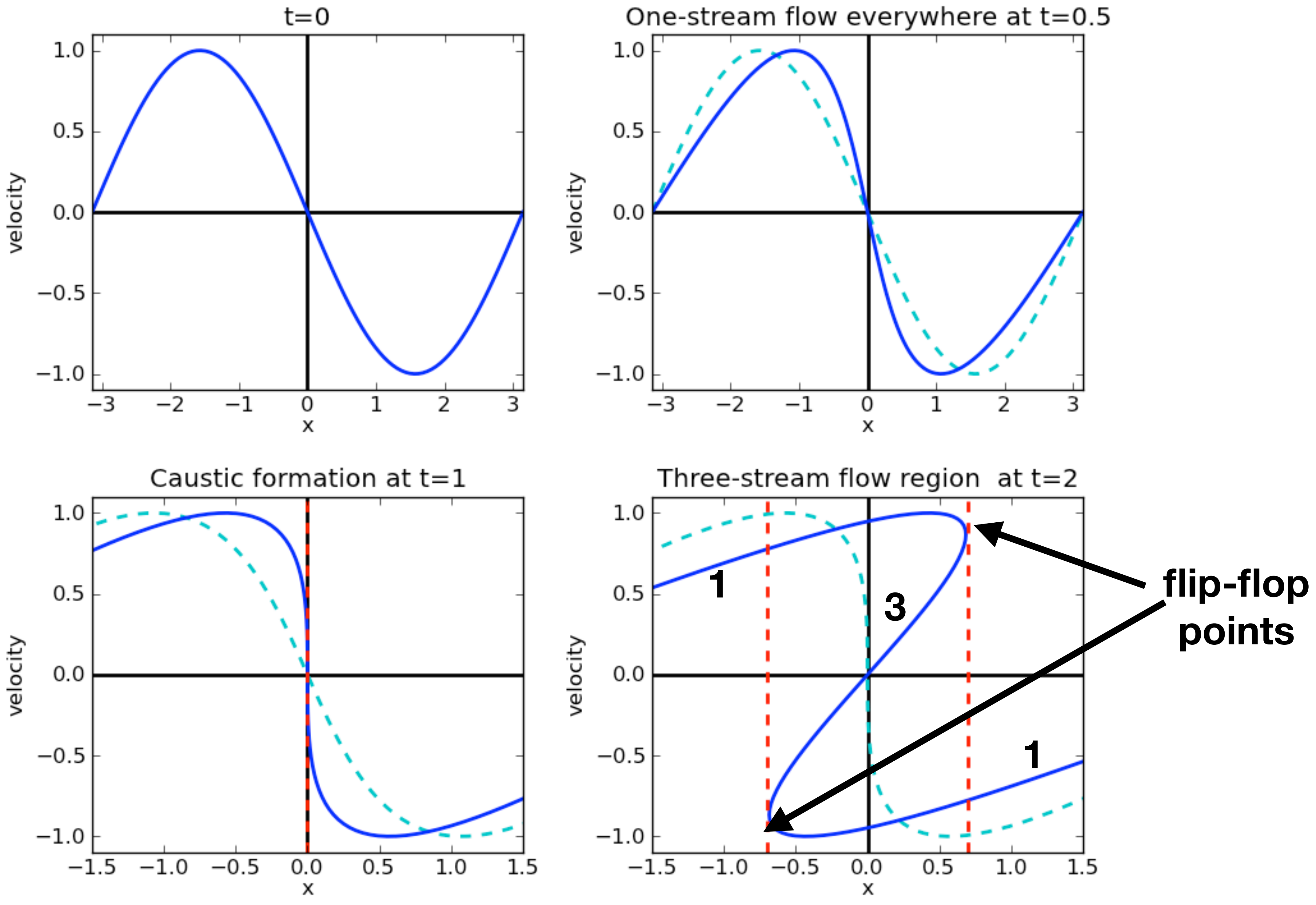

Density

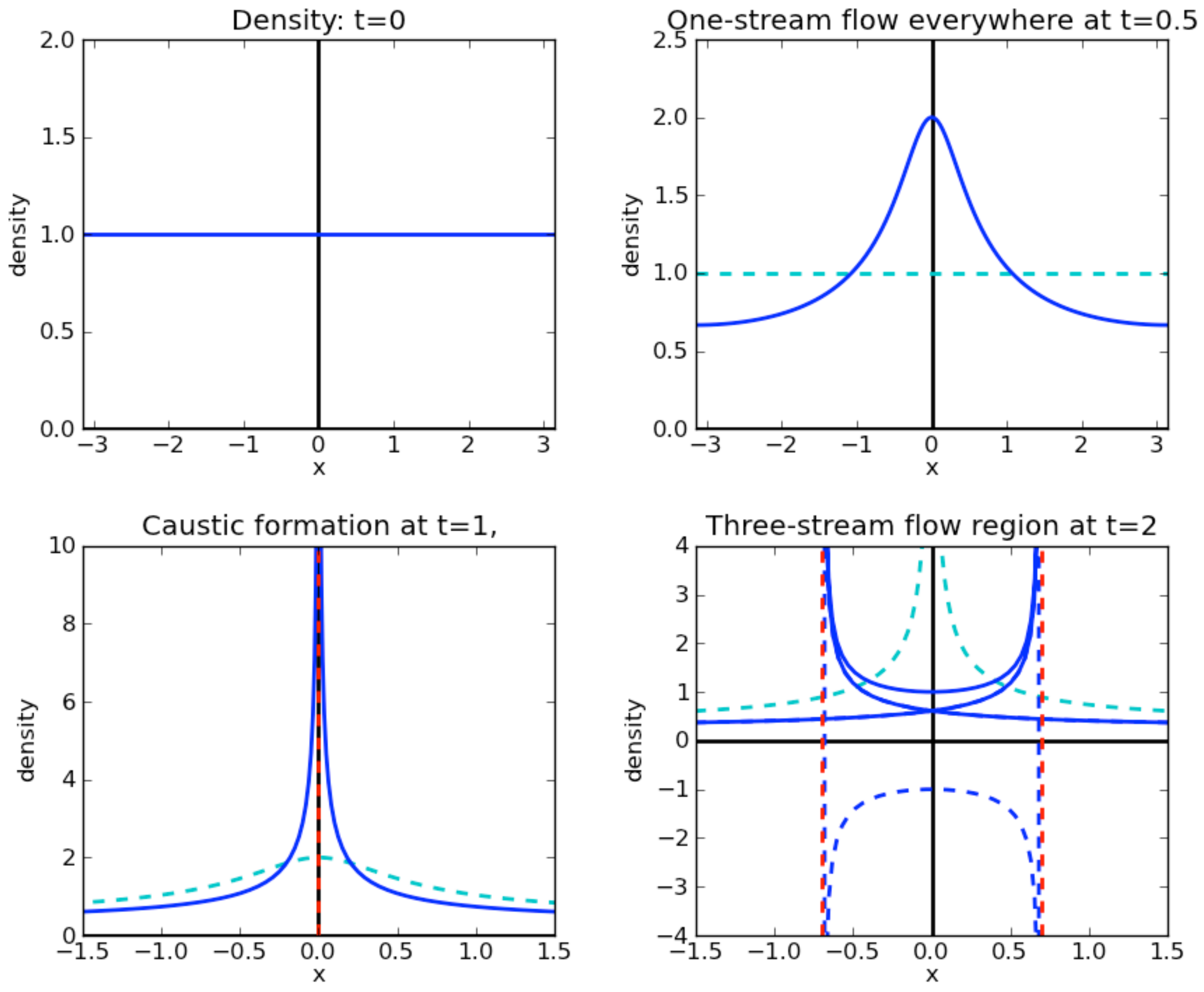

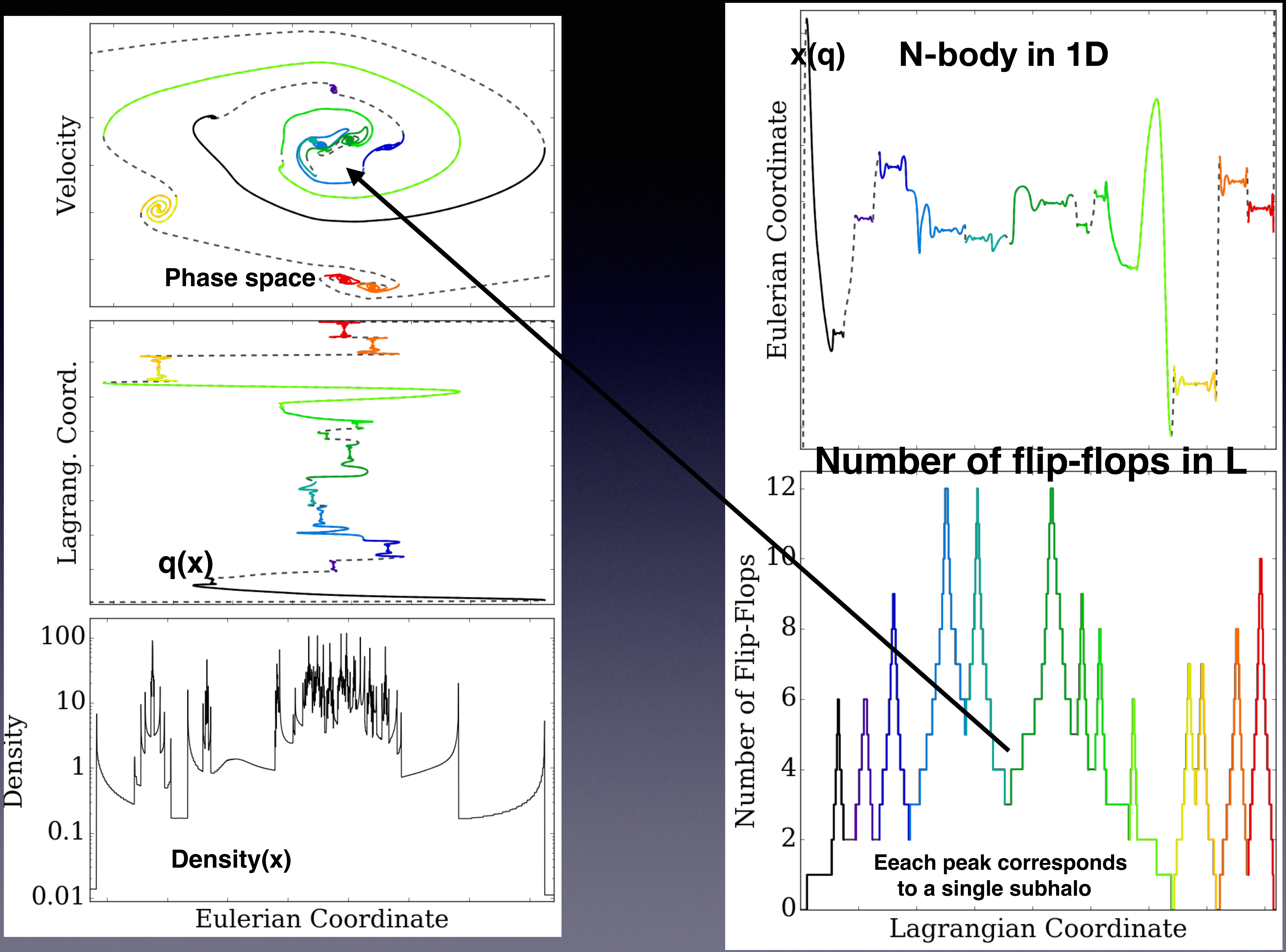

Velocity
Phase space
Lagrang. Coord.
q(x)
Density
Density(x)
100
10
1
0.1
0.01
Eulerian Coordinate
x(q)
N-body in 1D
Eulerian Coordinate
Number of flip-flops in L
Number of Flip-Flops
12
10
8
6
4
2
0
Eeach peak corresponds
to a single subhalo
Lagrangian Coordinate

L-space ZA E-space in 2D

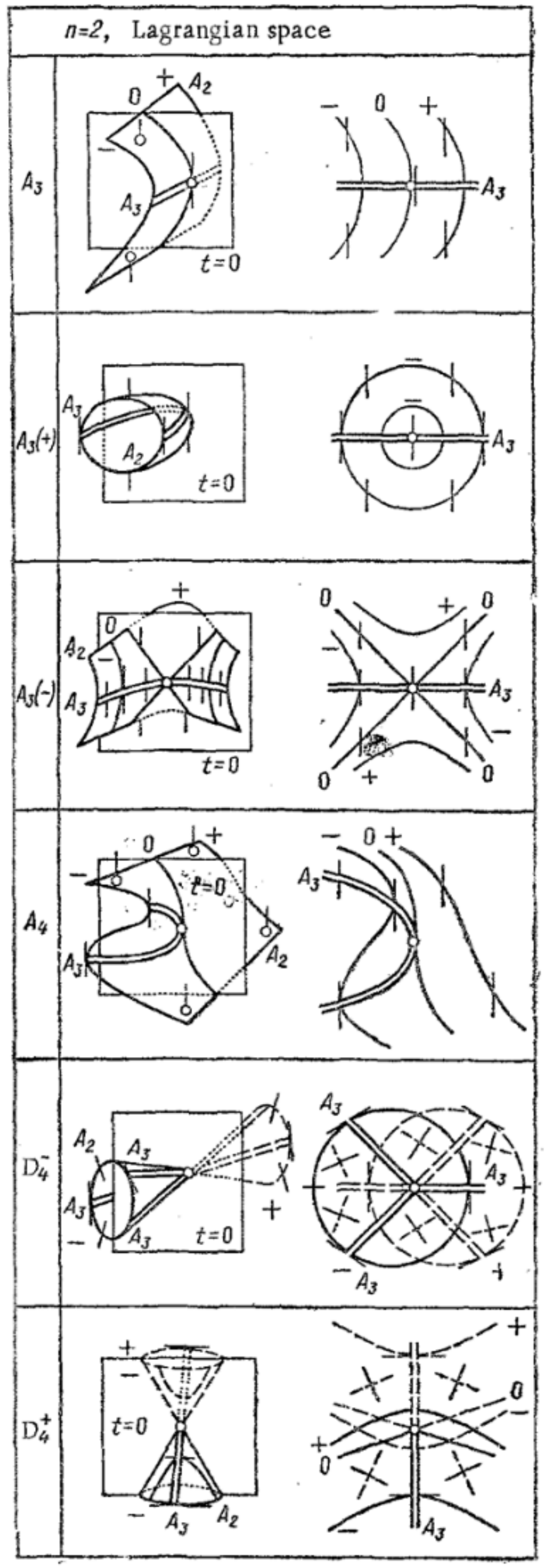

Fig. 4

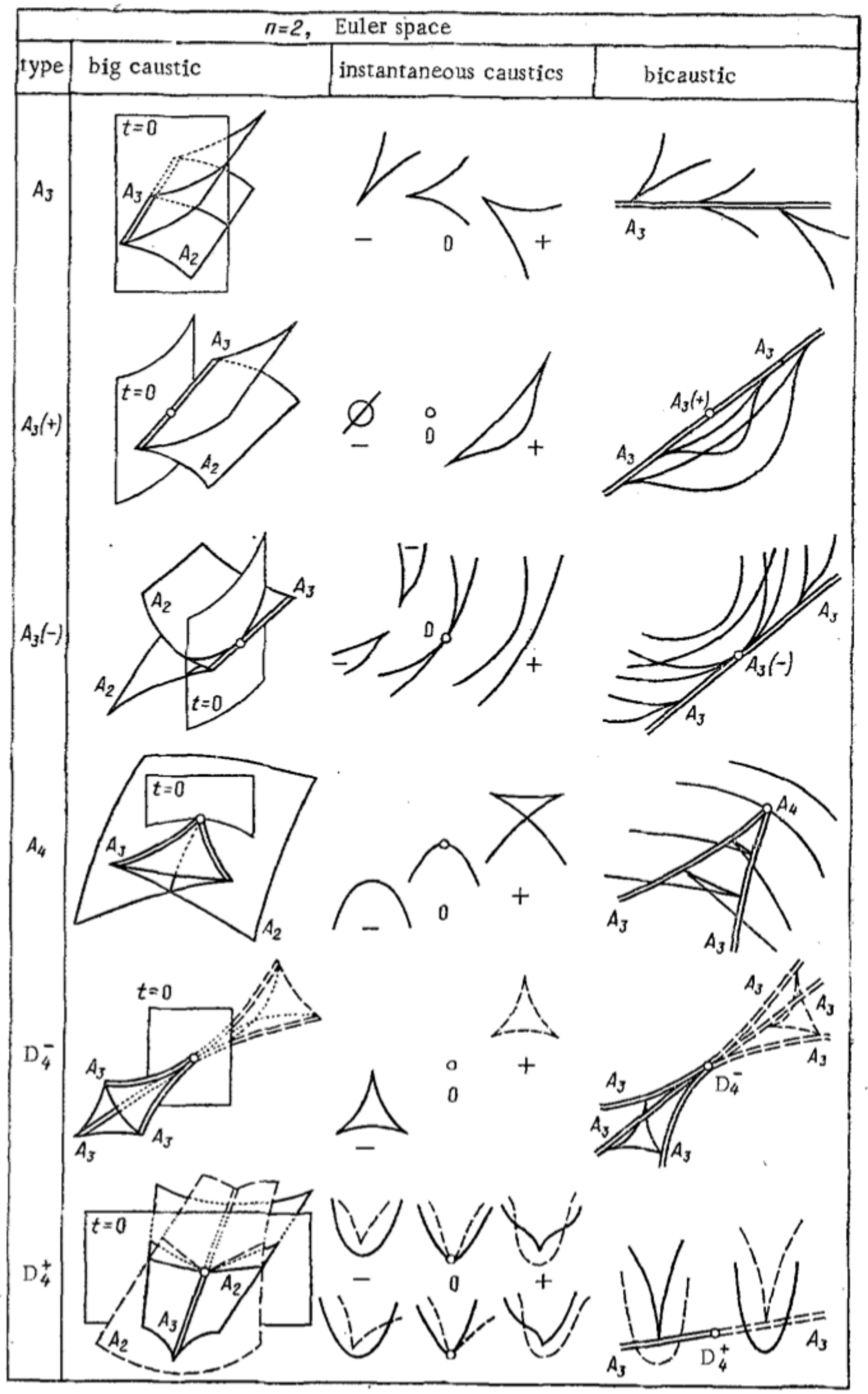

Fig. 3

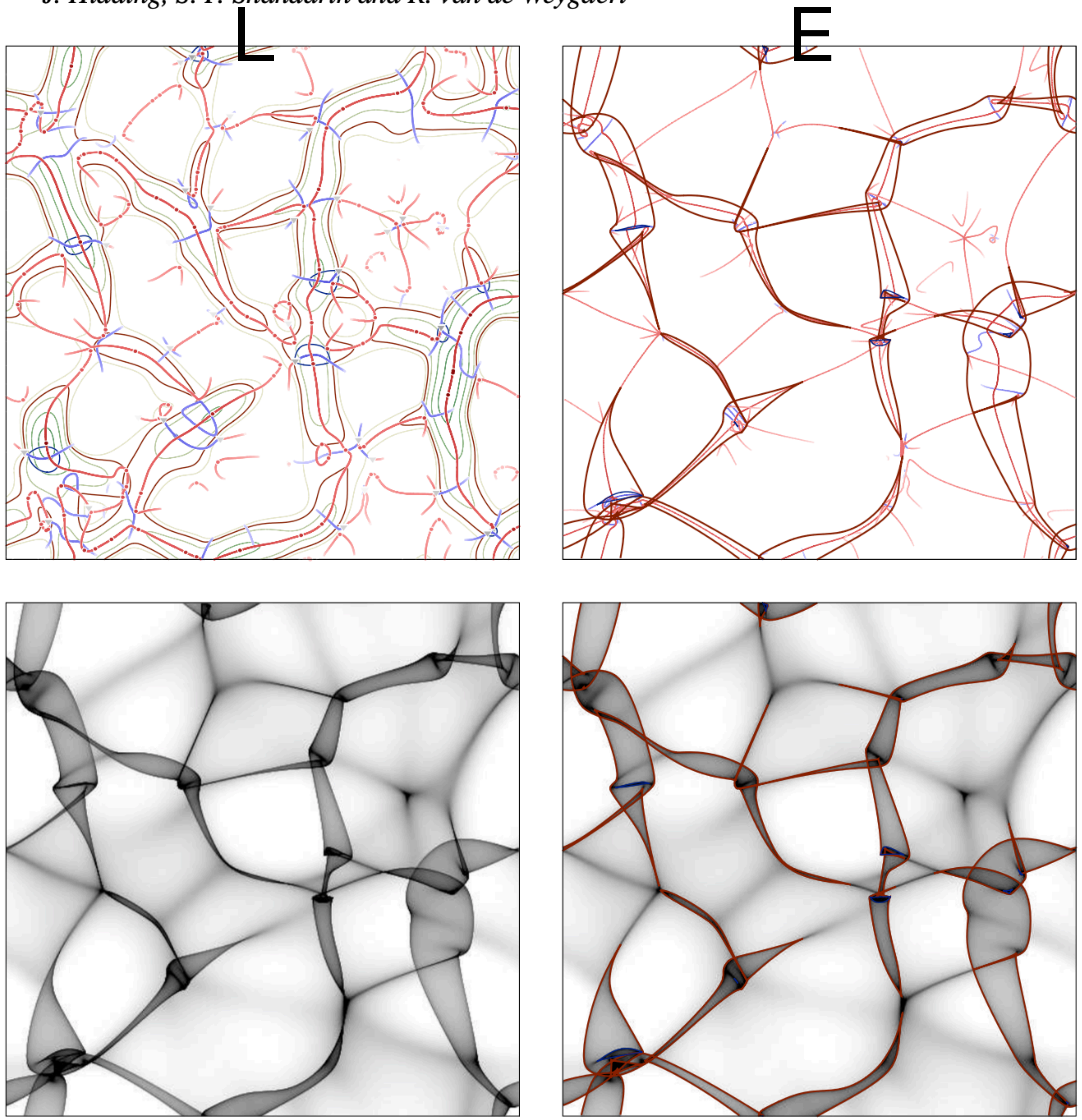

Figure 1. ZA: Lagrangian and Eulerian singularity structure. First panel: the Lagrangian skeleton that we find using the method presented in this paper. In dark red is the contour of the major eigenvalue corresponding to the time at which we plotted the Eulerian images that occupy the other three panels. Top-right panel: structural and singularity information from the first panel mapped to Eulerian space, as proscribed by the ZA. Bottom-left panel: density distribution in Eulerian space. Bottom-right panel: density field in Eulerian space, with the singularity outline superimposed (red edges).

Castics in 2D N-body simulations
Melott, Shandarin 1989

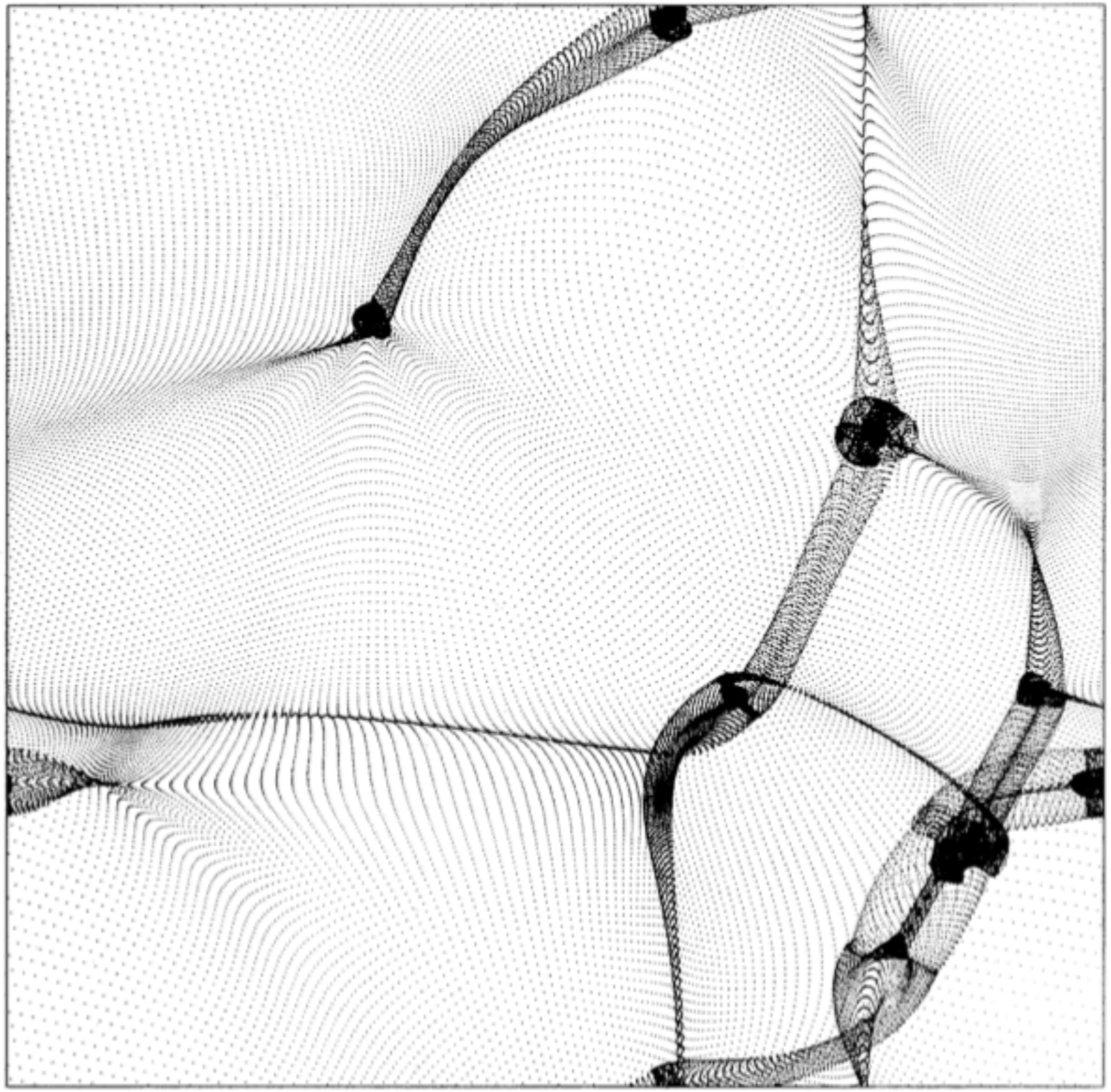

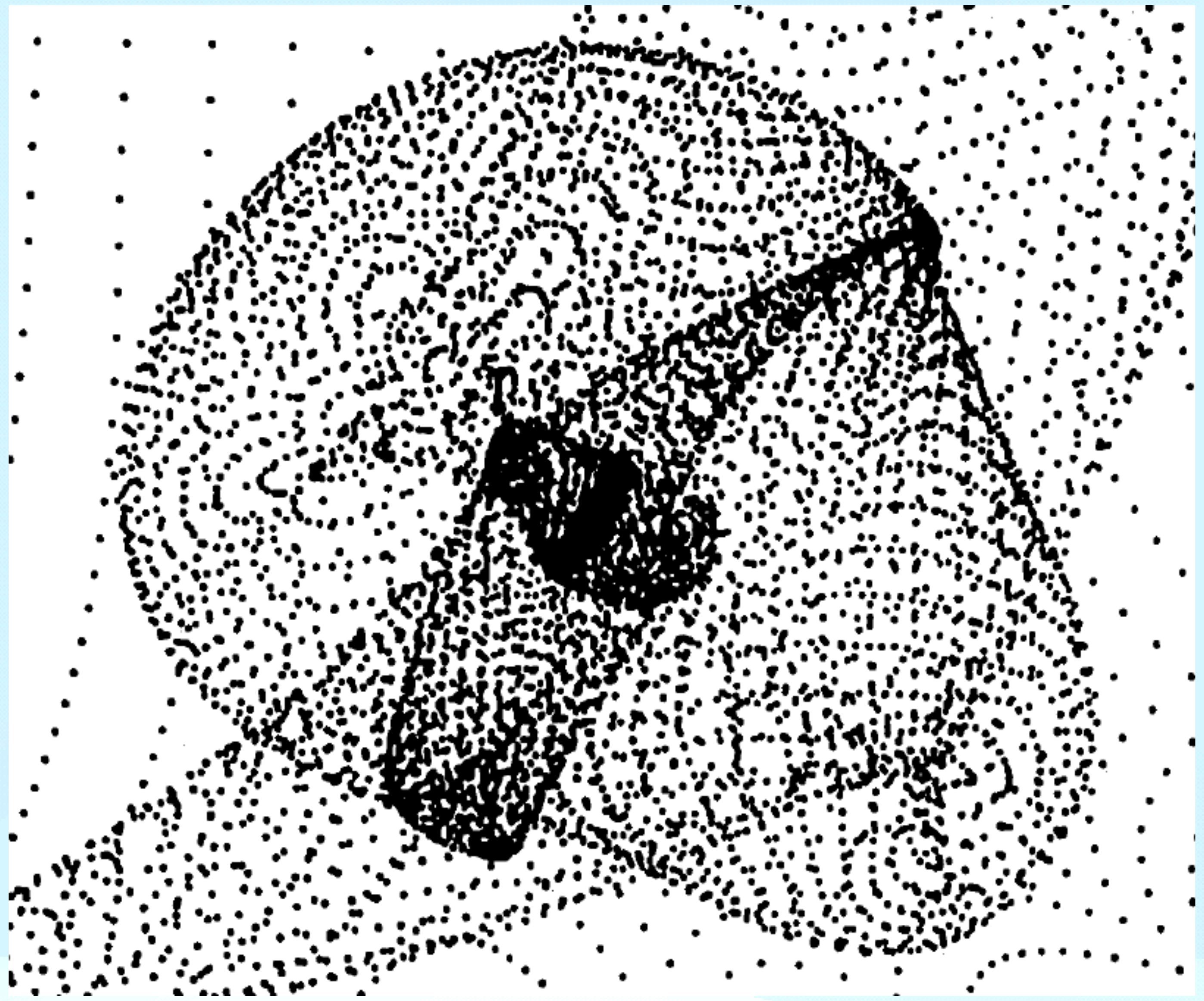

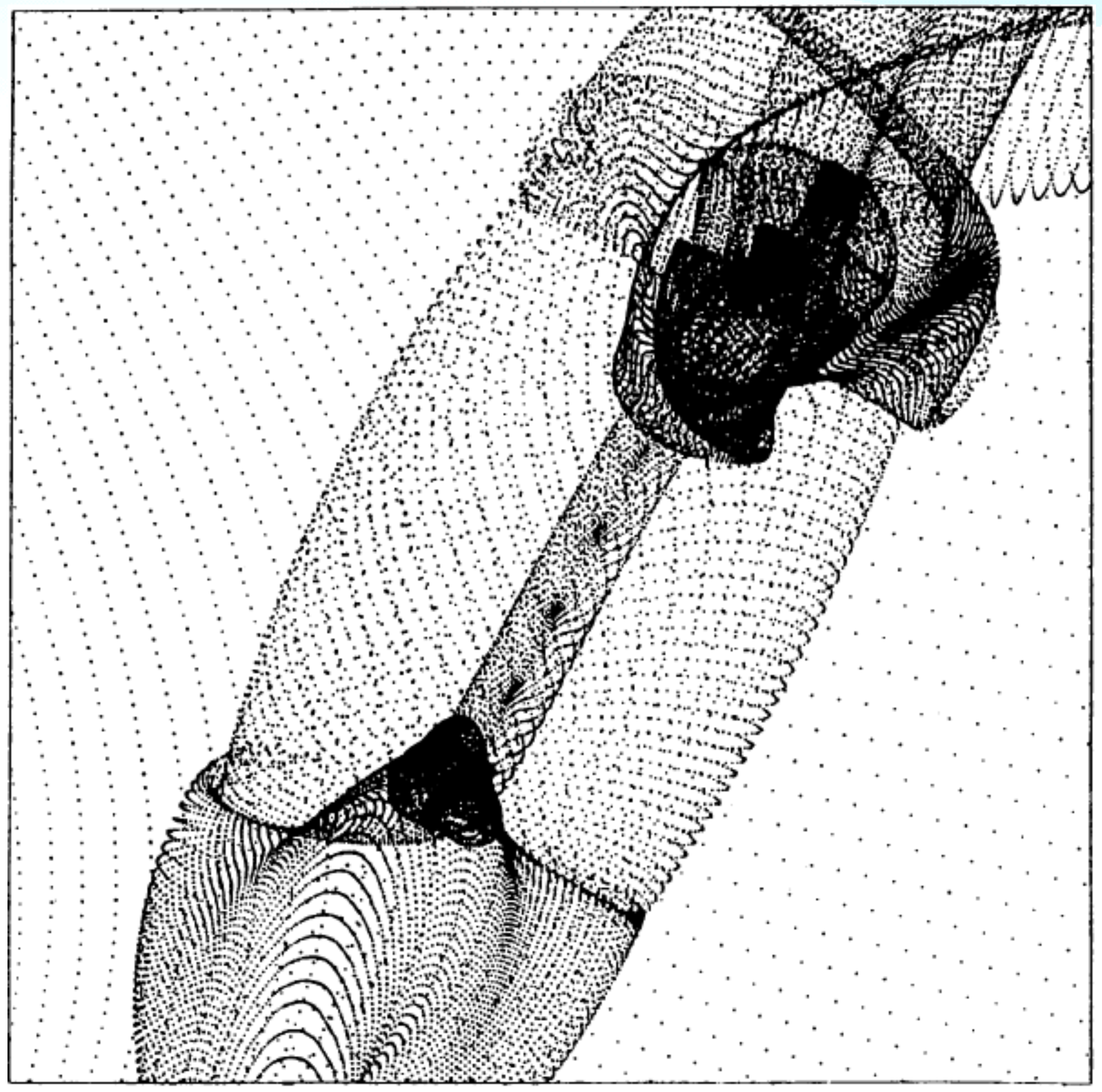

ZA E-space A - caustics in 3D Arnold 1982

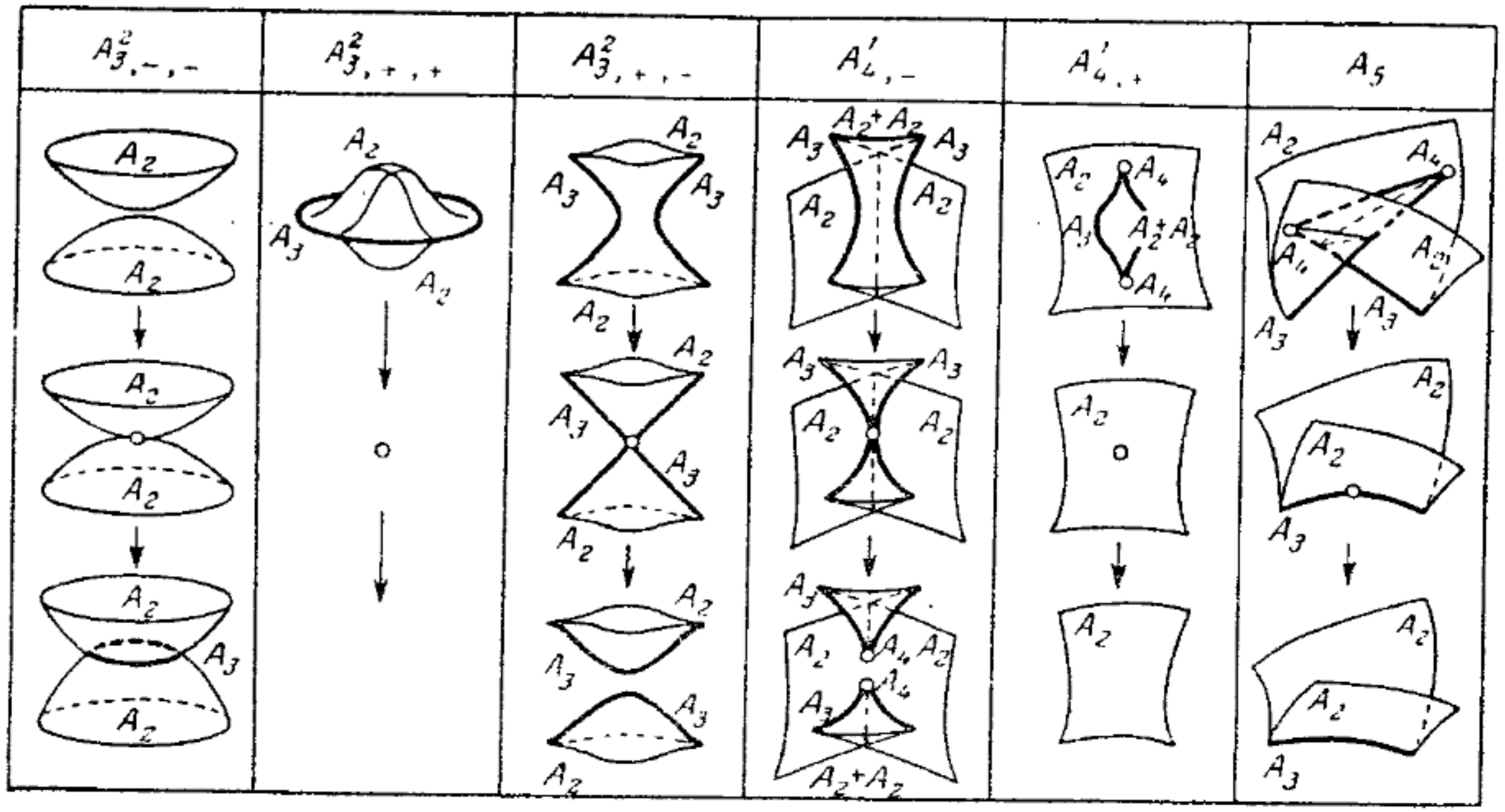

D - caustics in 3D

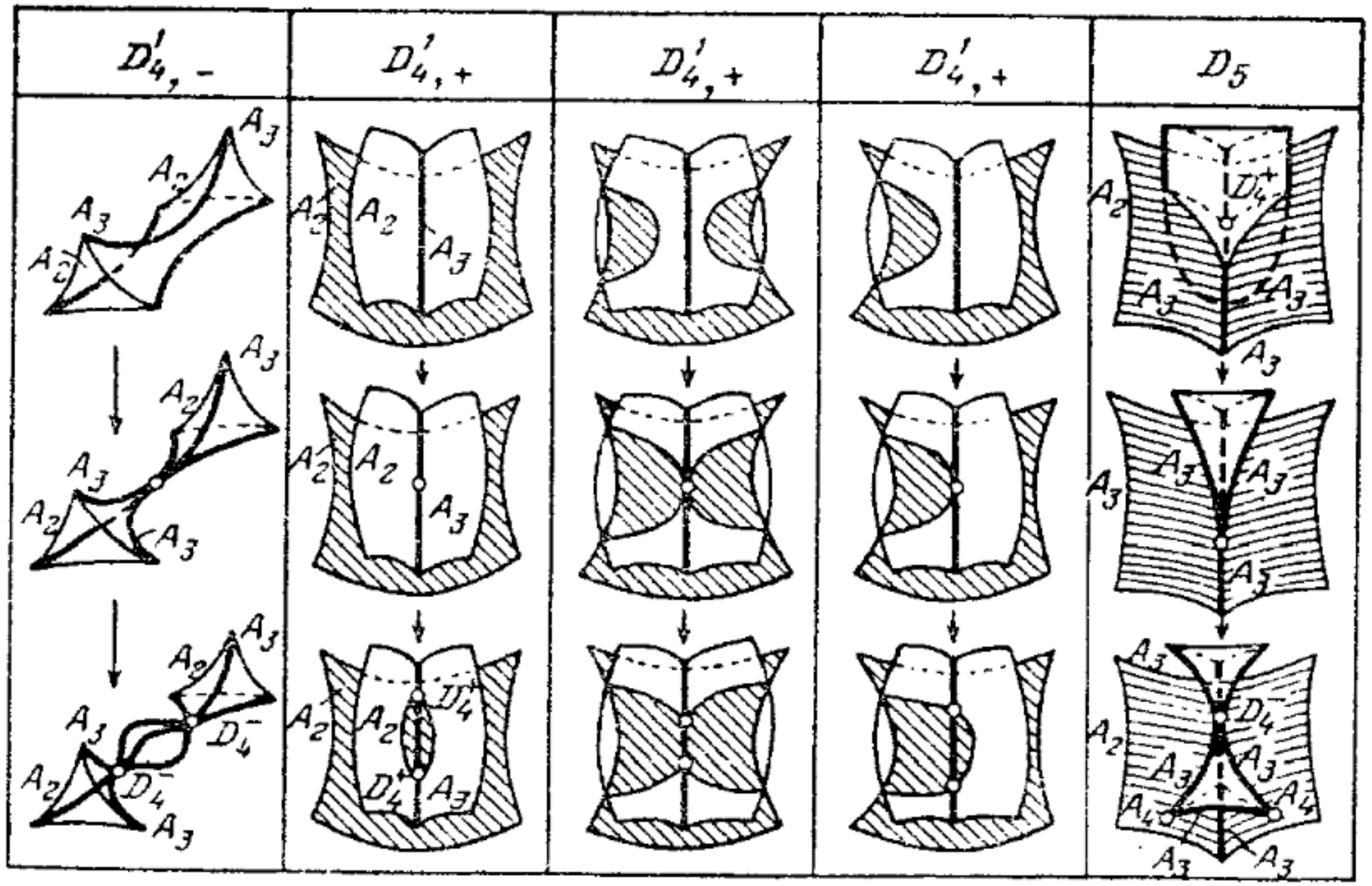

Caustics in 3D

J. Hidding, S. F. Shandarin and R. van de Weygaert

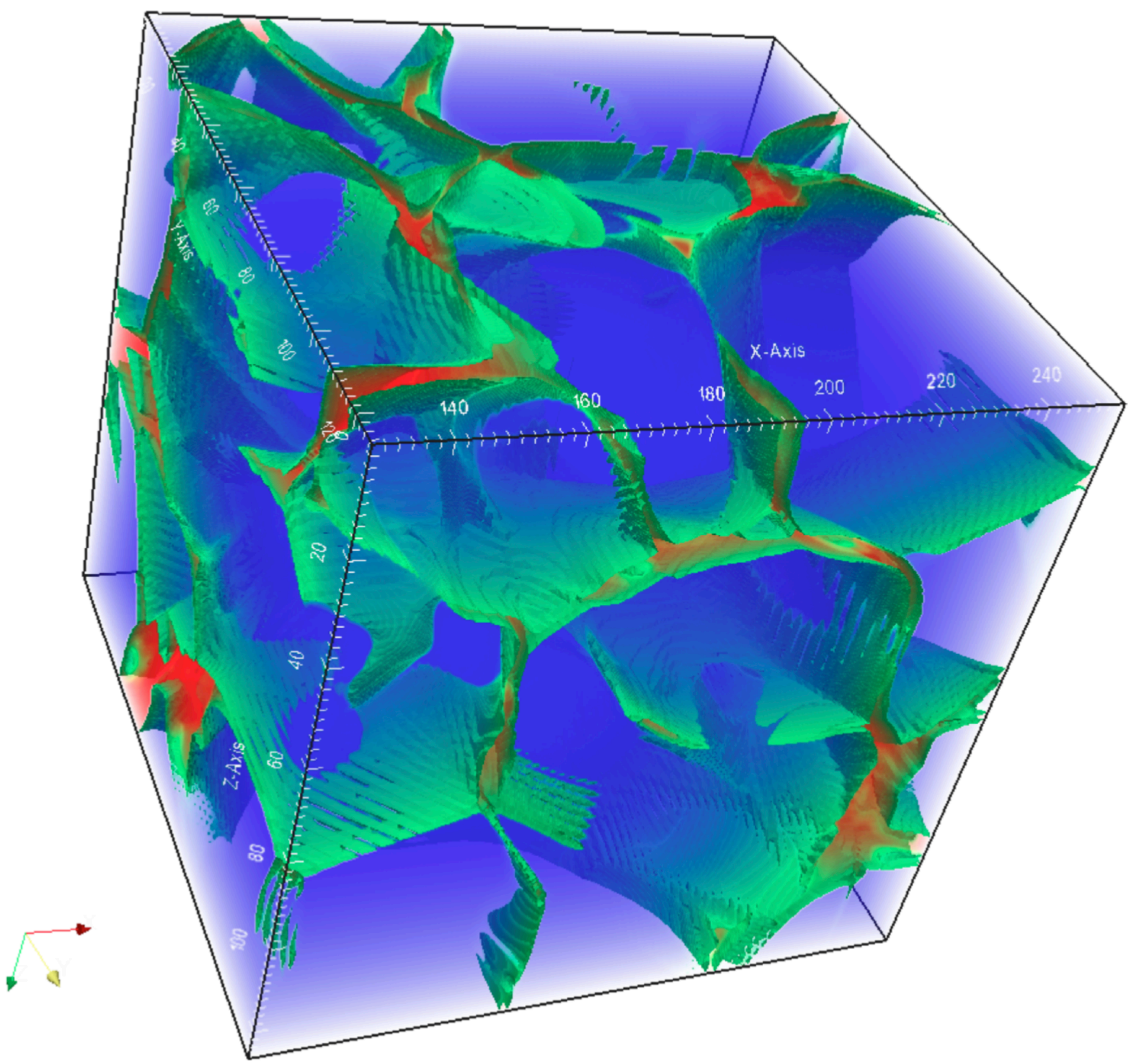

Caustic Structure of Filaments and Halos

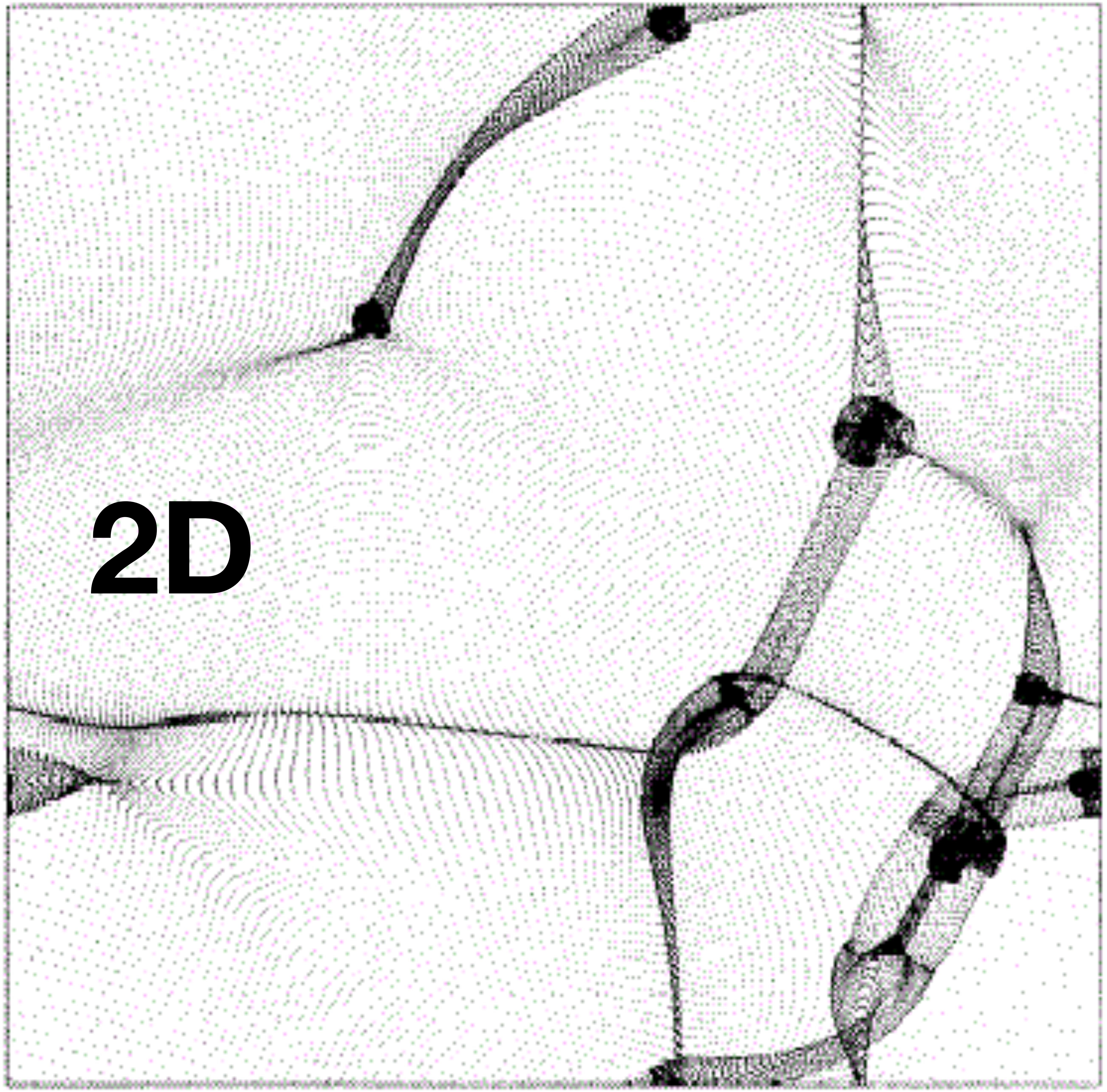

Melot, Shandarin 1989

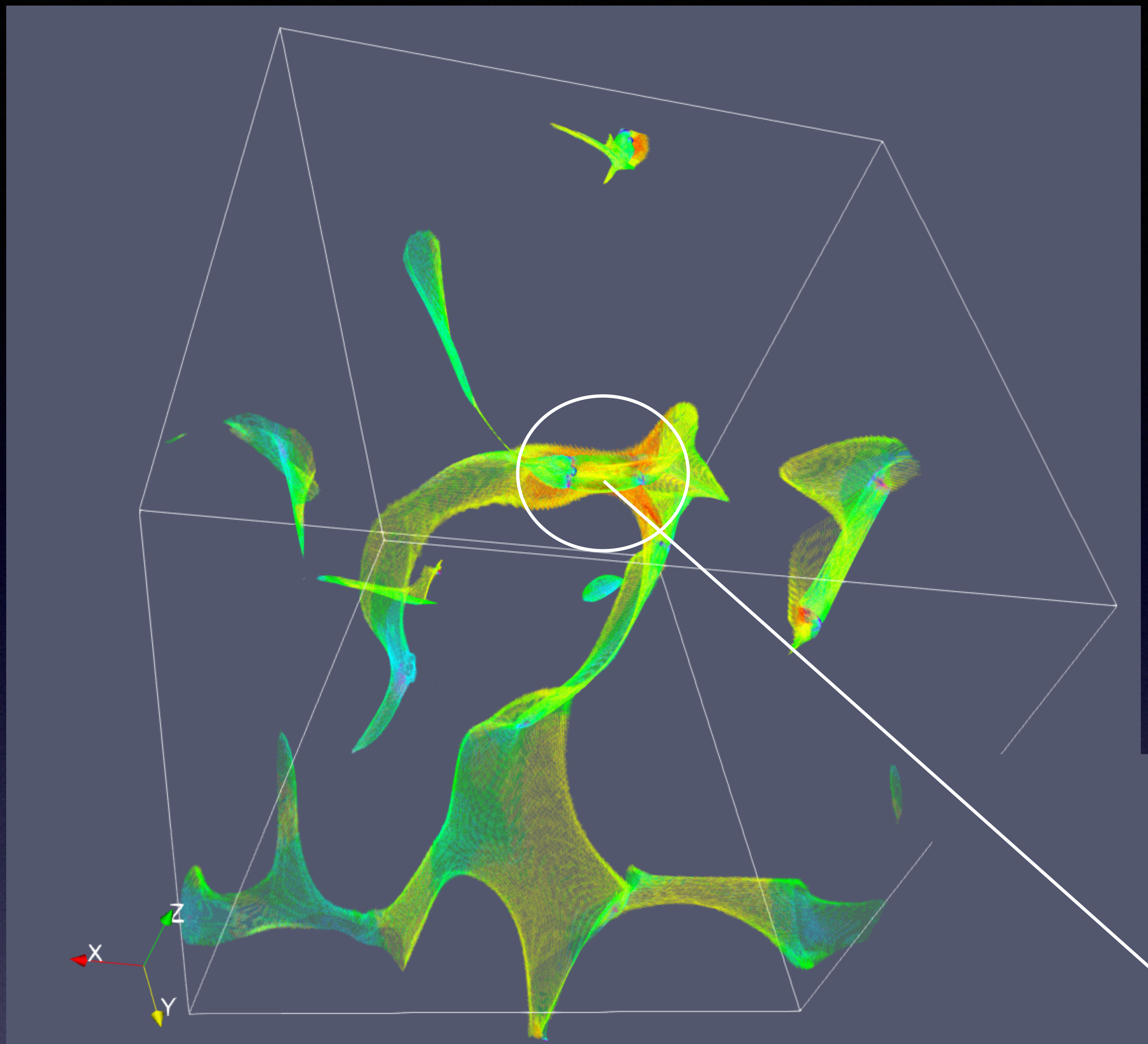

N-body simulation:
Np=256^3,   L=100/h Mpc
Force res.=0.8/h Mpc
k_cutoff = 4 (2pi / L)
R_sphere = 20 Mpc/h

Shandarin 2021

Flip-flop :
Change of sign of
det(dx_i/dq_j)

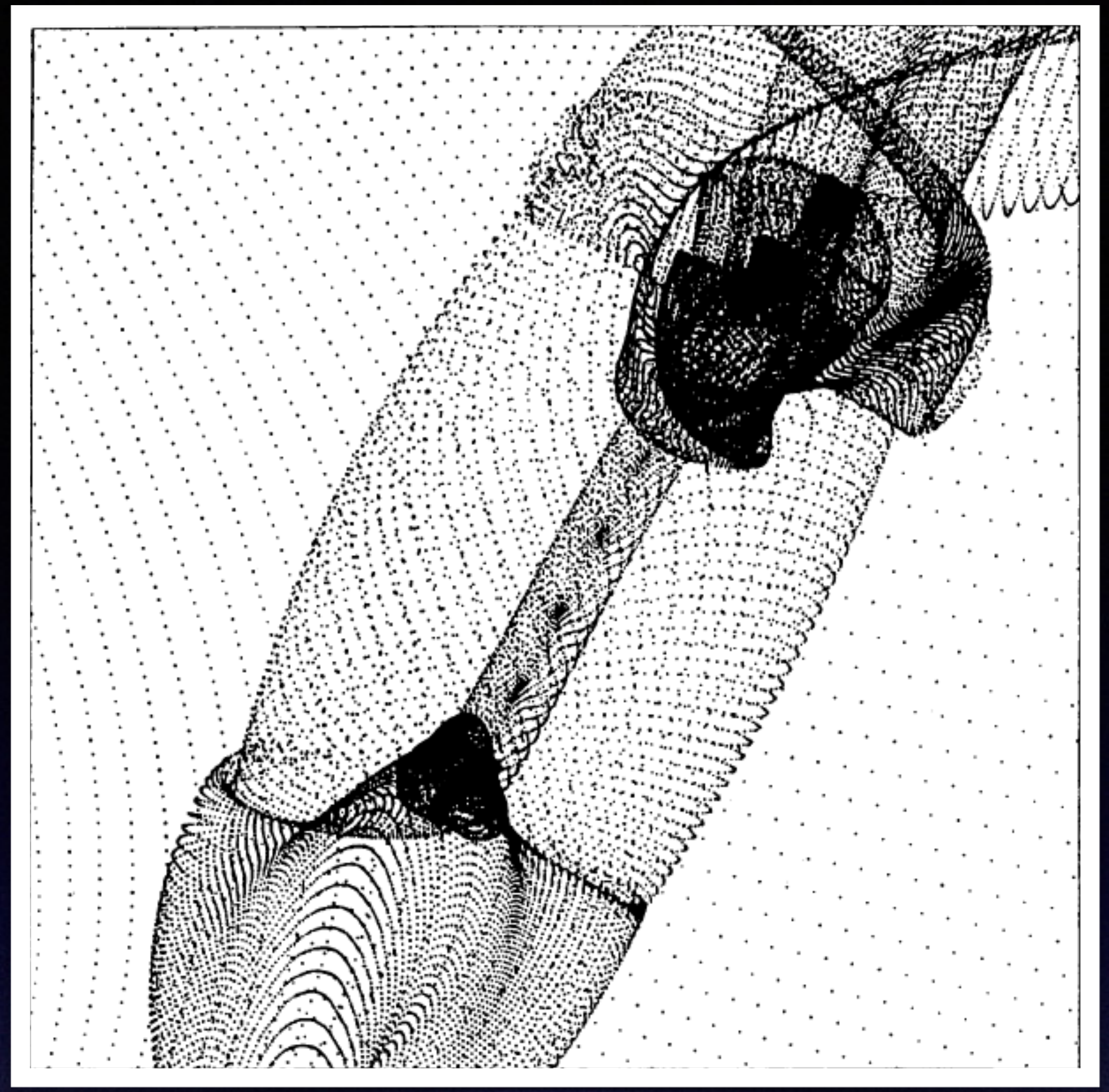

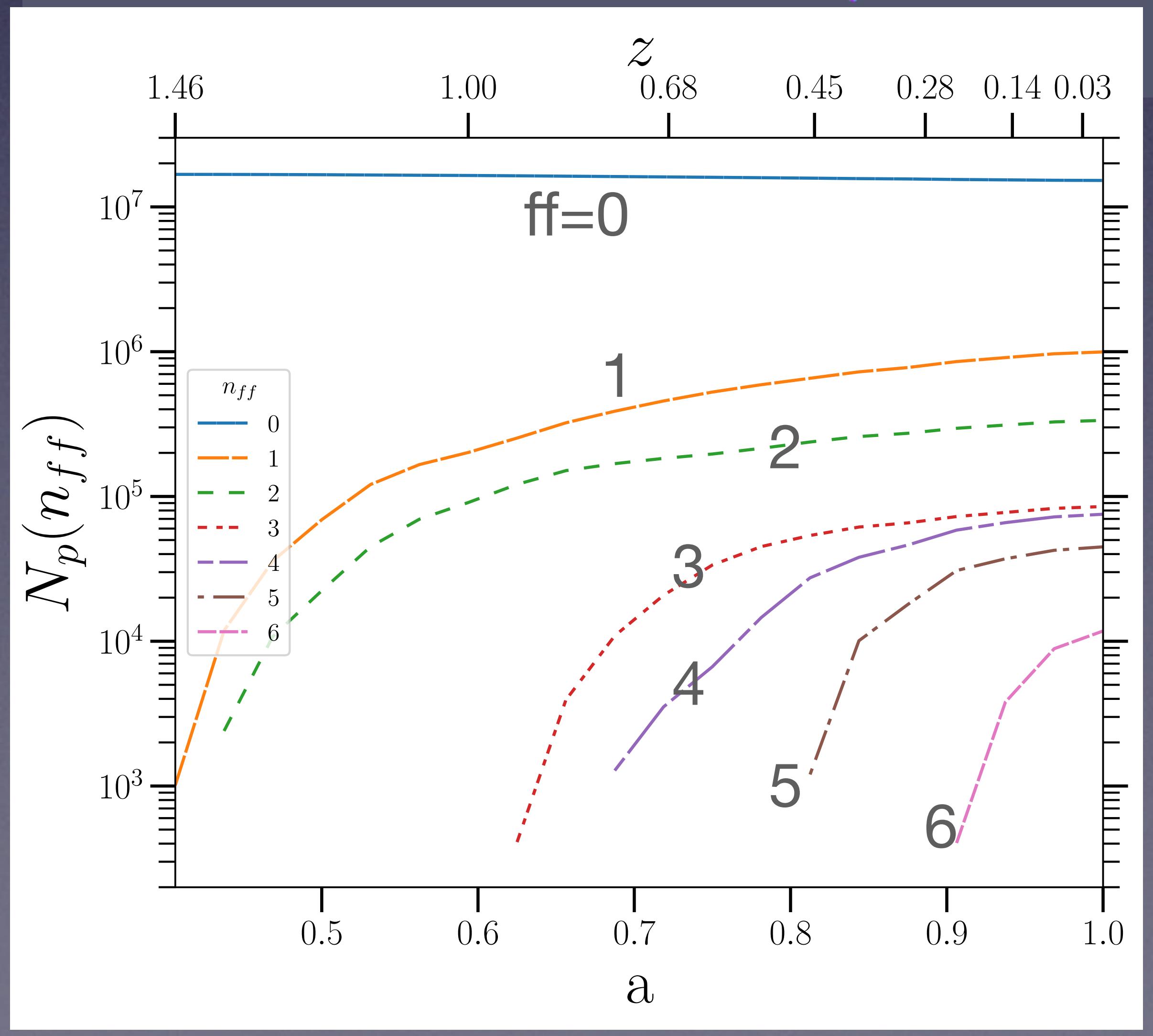

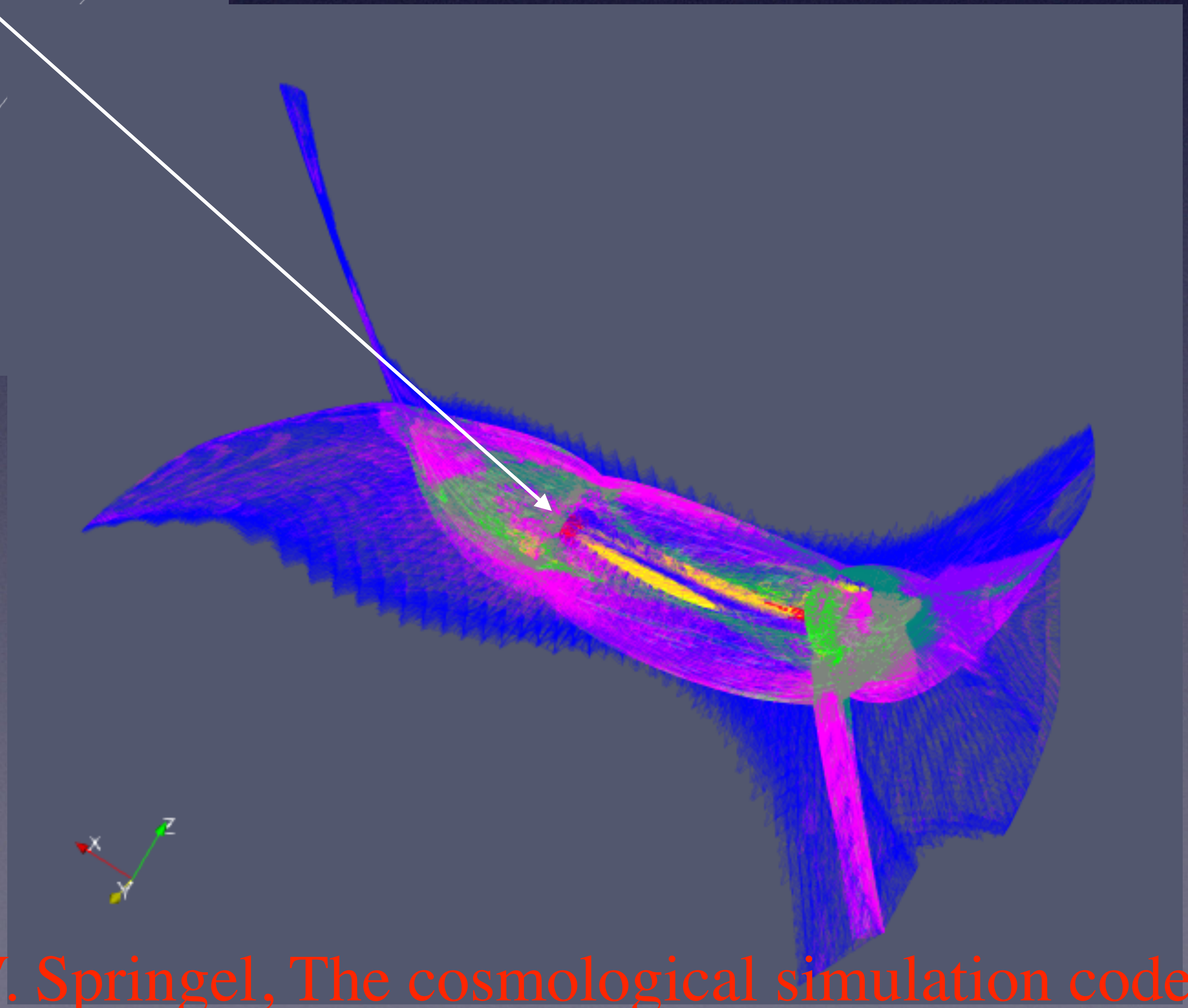

- V. Springel, The cosmological simulation code GADGET-2

Particles in 3D with number of flip-flops > 0

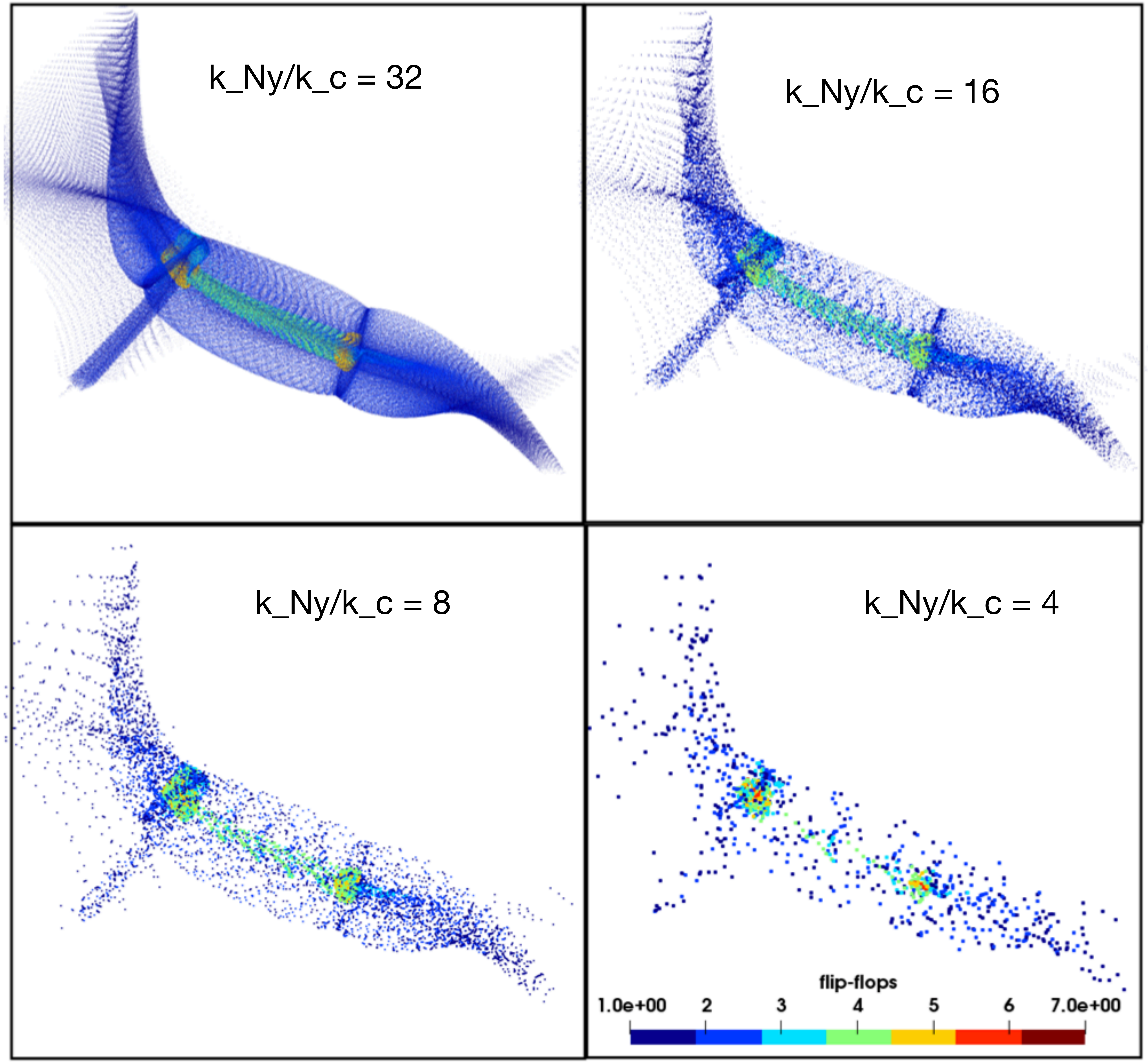

Five distinct components (blue, magenta, green, yellow, and red) of the central caustic structure shown in bottom right of the previous slide

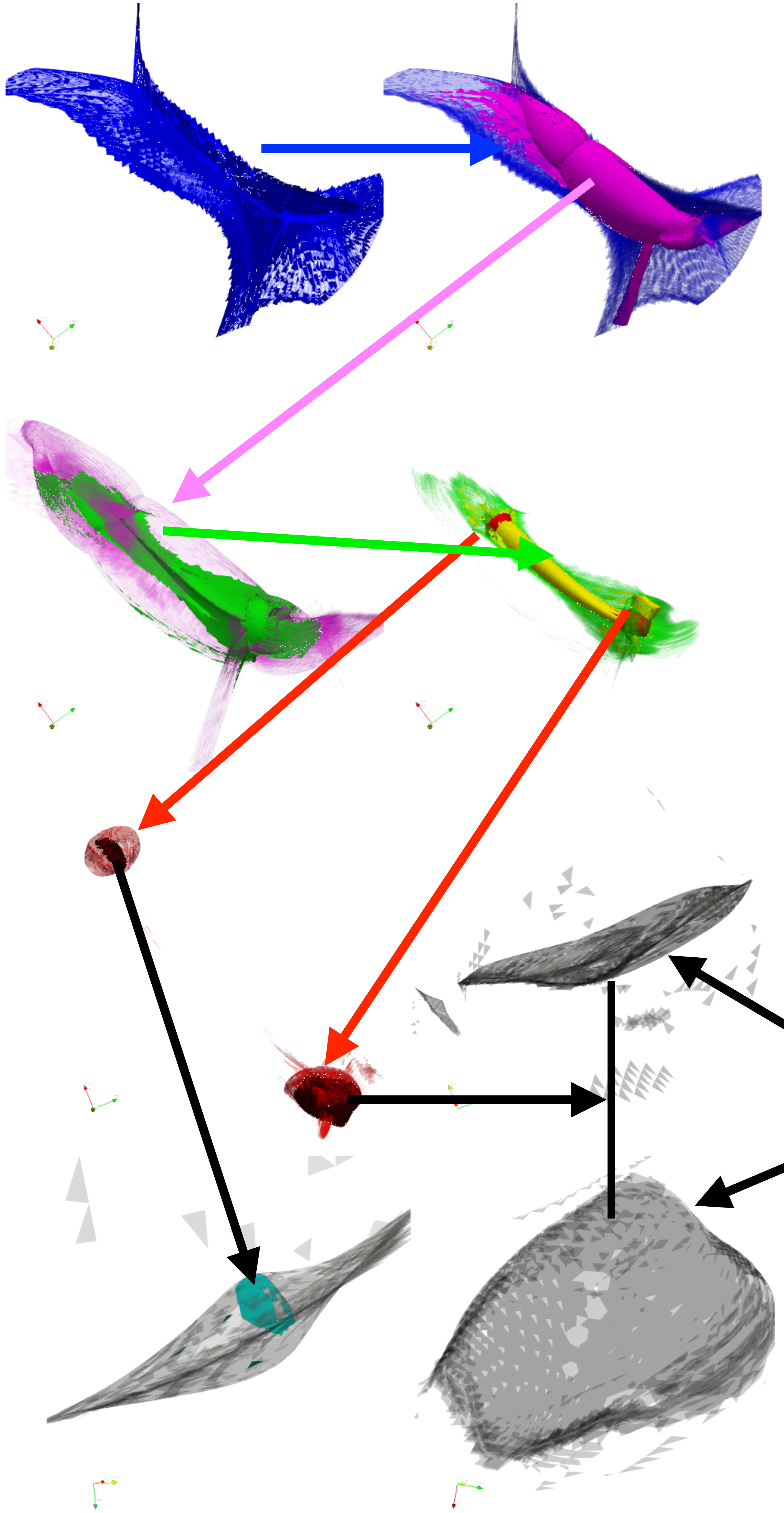

Caustics (in gray) inside of two red caustics

two orthogonal projections

Slice by a plane through two convex red caustic shells

Eulerian space

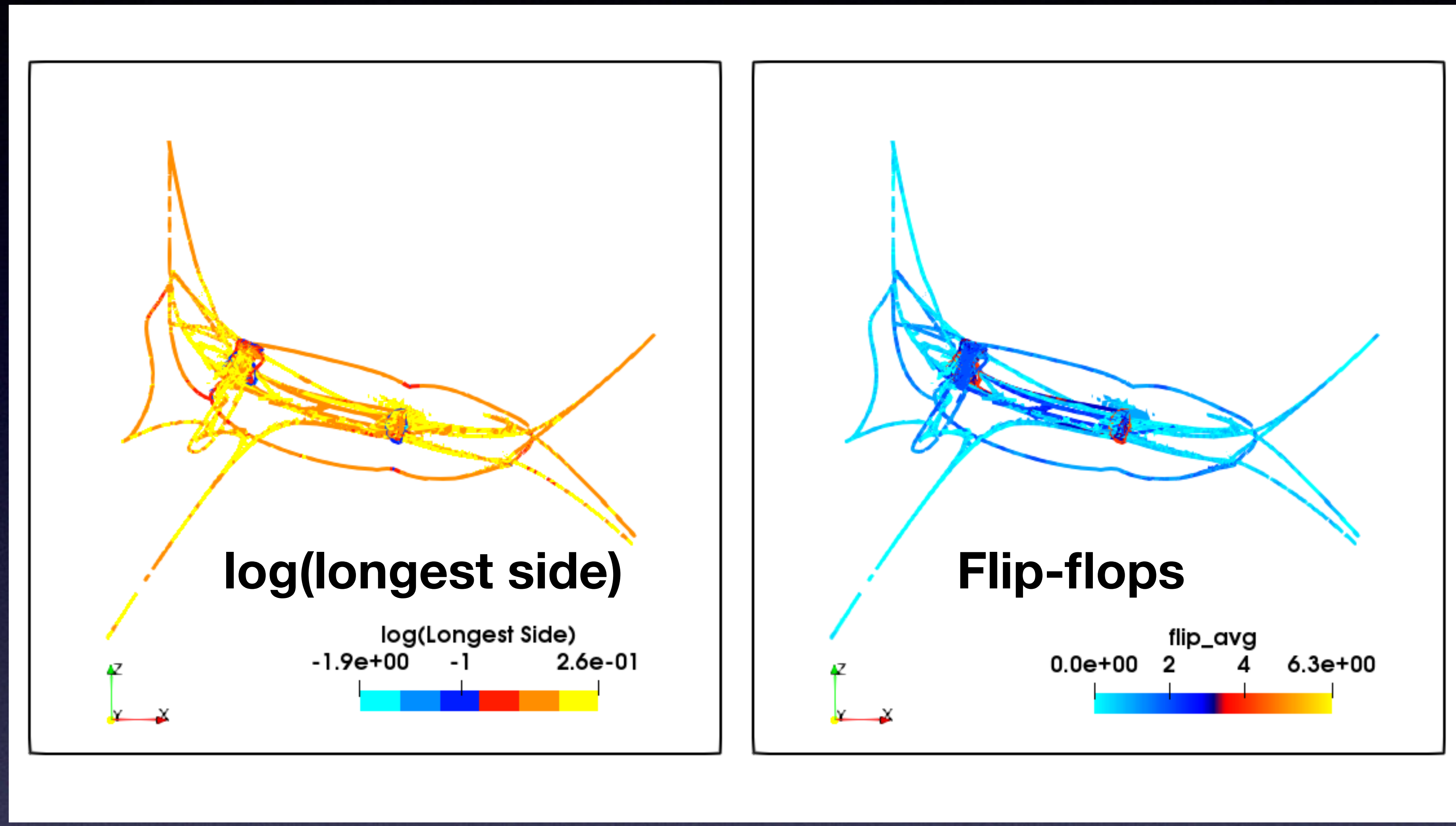

Lagrangian space

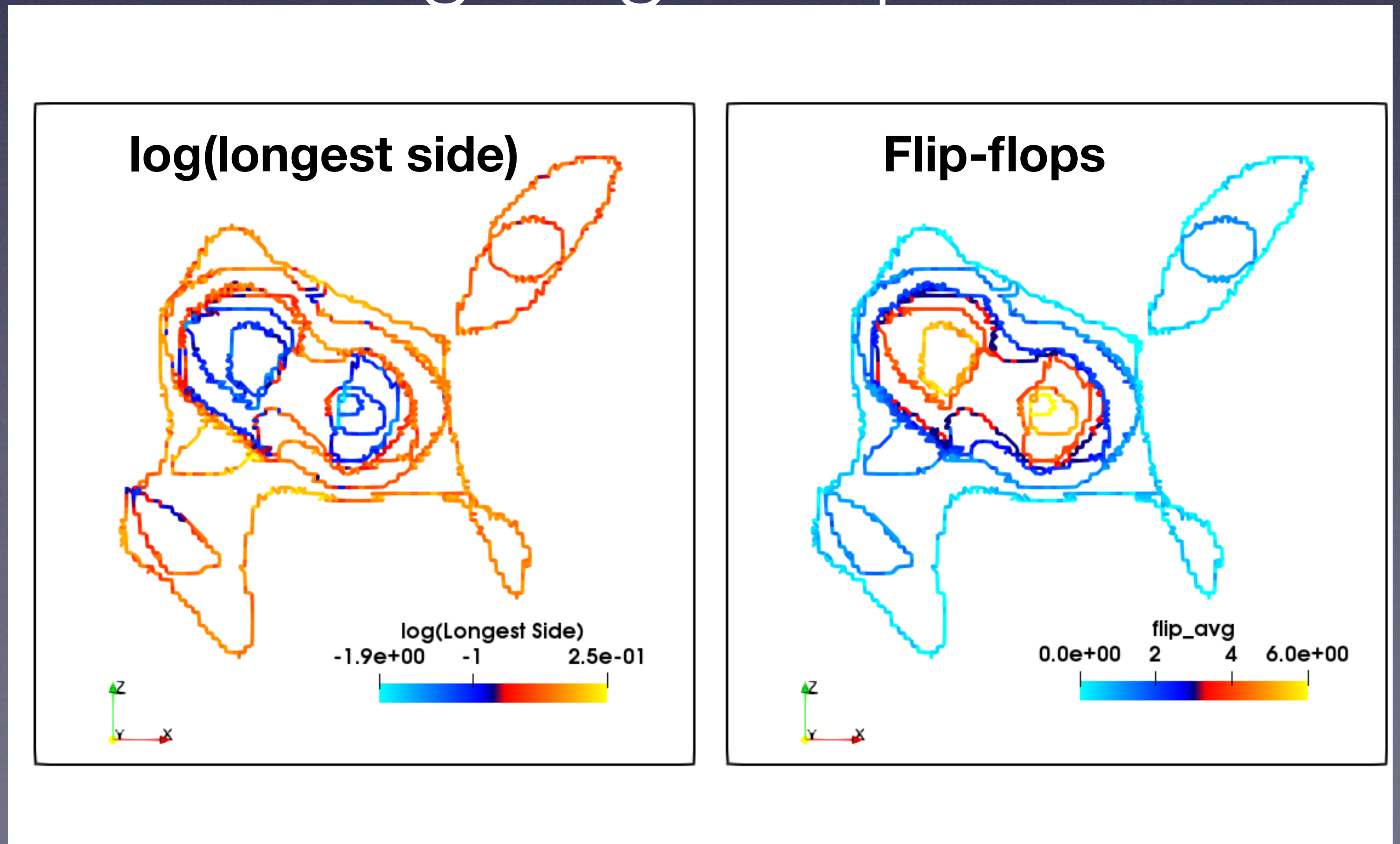

Slice by an orthogonal plane through the middle of the structure

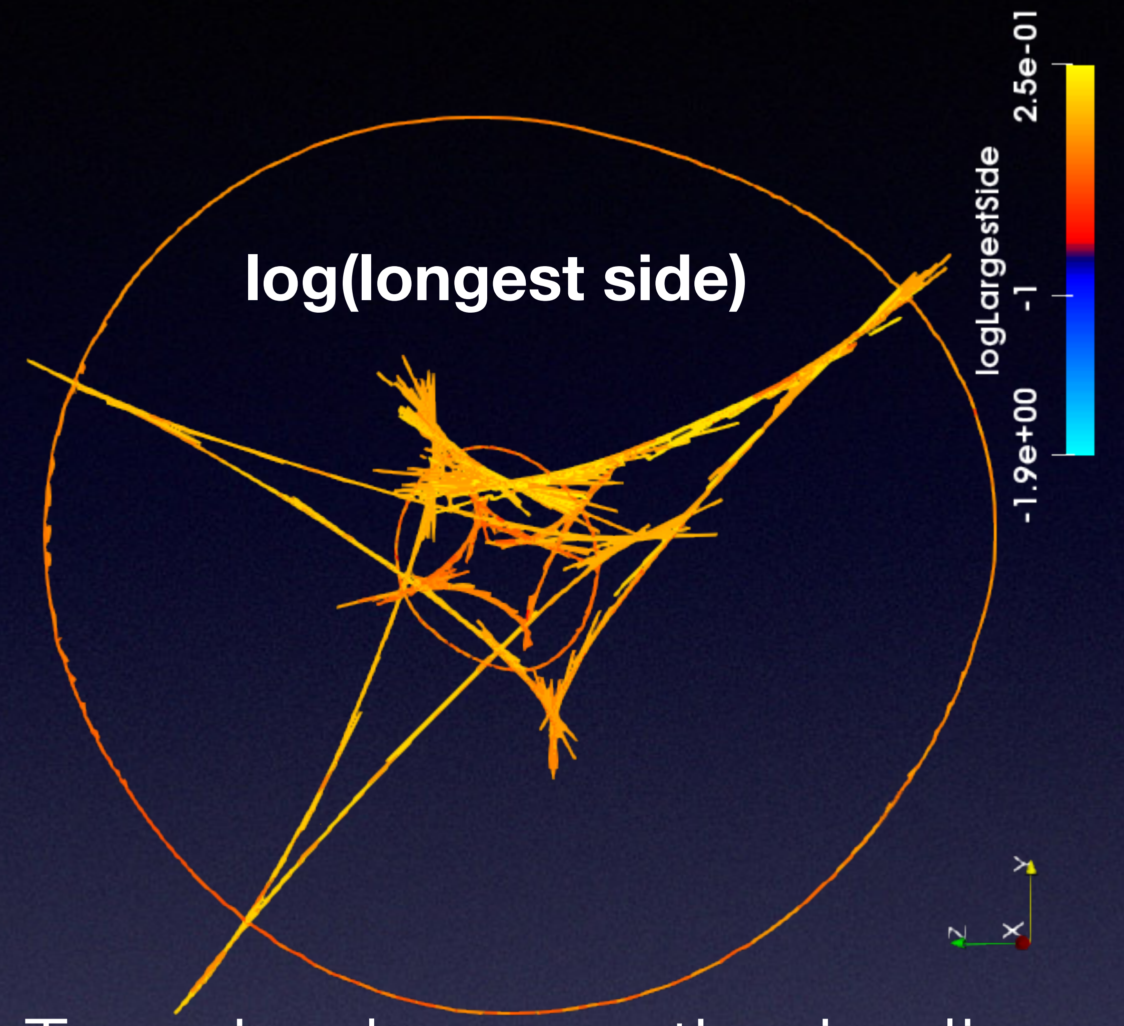

Two circular caustics in slice
(do not exist in Zeldovich approximation)

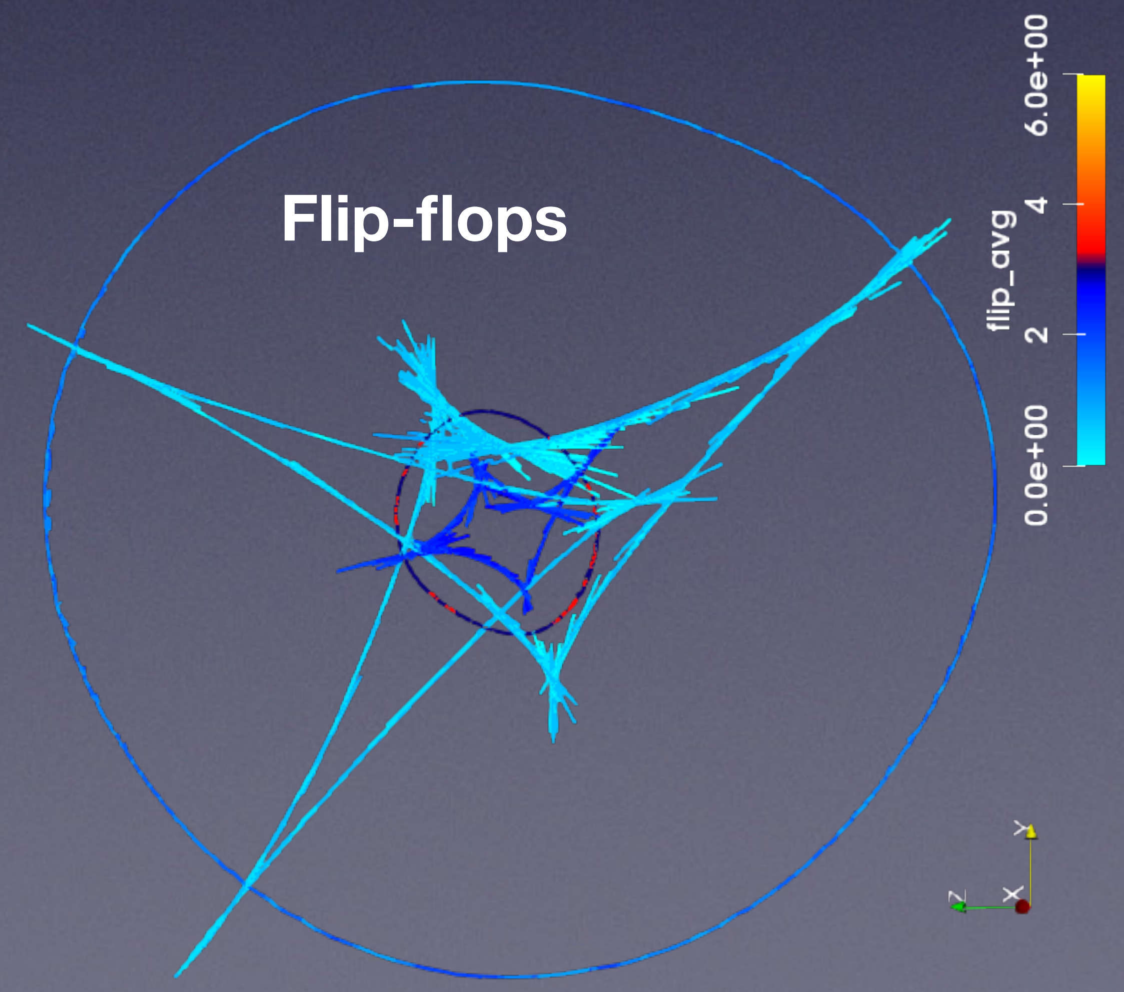

Slice by a plane through two convex red caustic shells

Slice by an orthogonal plane through the middle of the structure

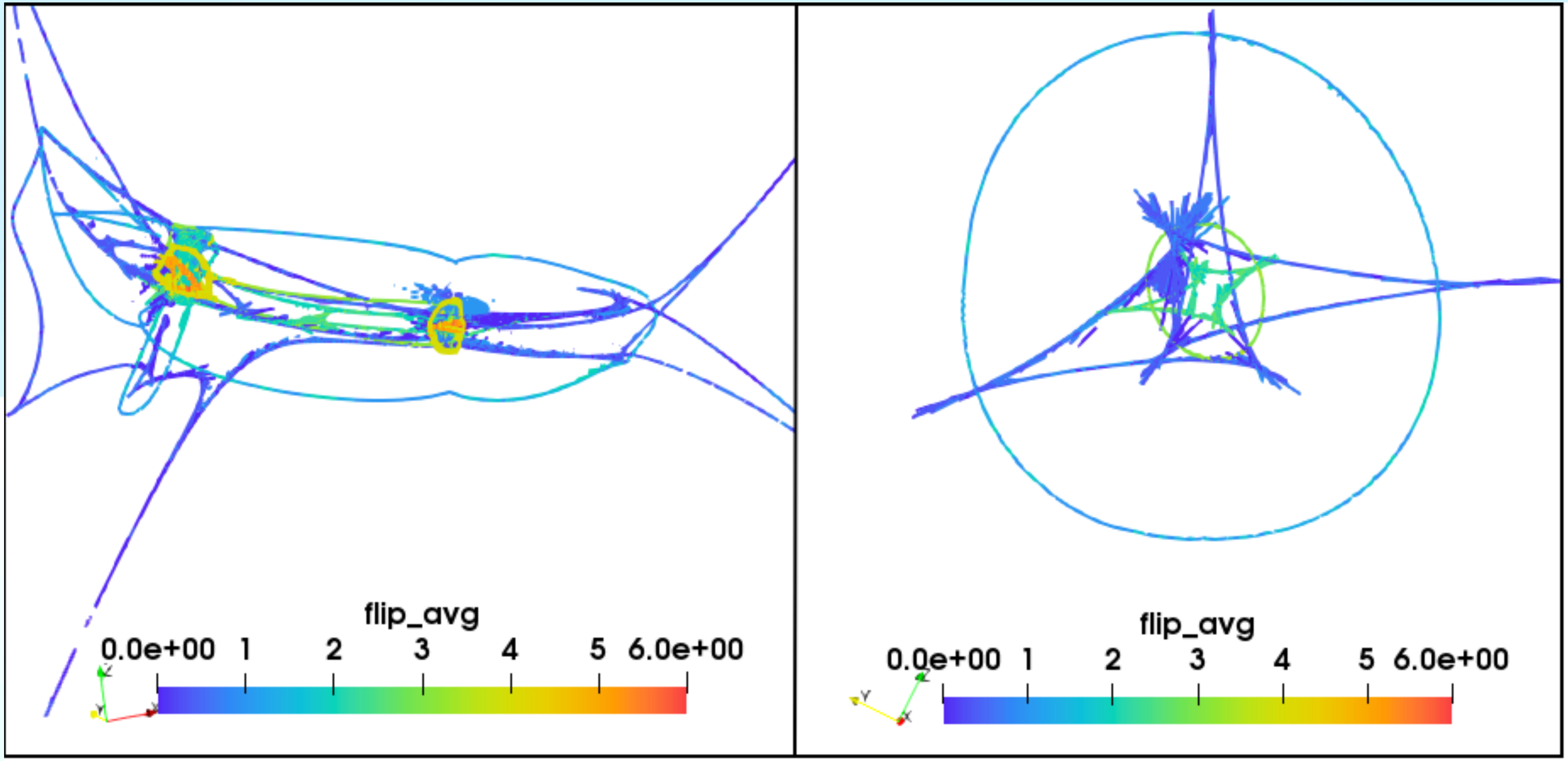

Eulerian space

Slice by a plane through two convex red caustic shells

Slice by an orthogonal plane through the middle of the structure

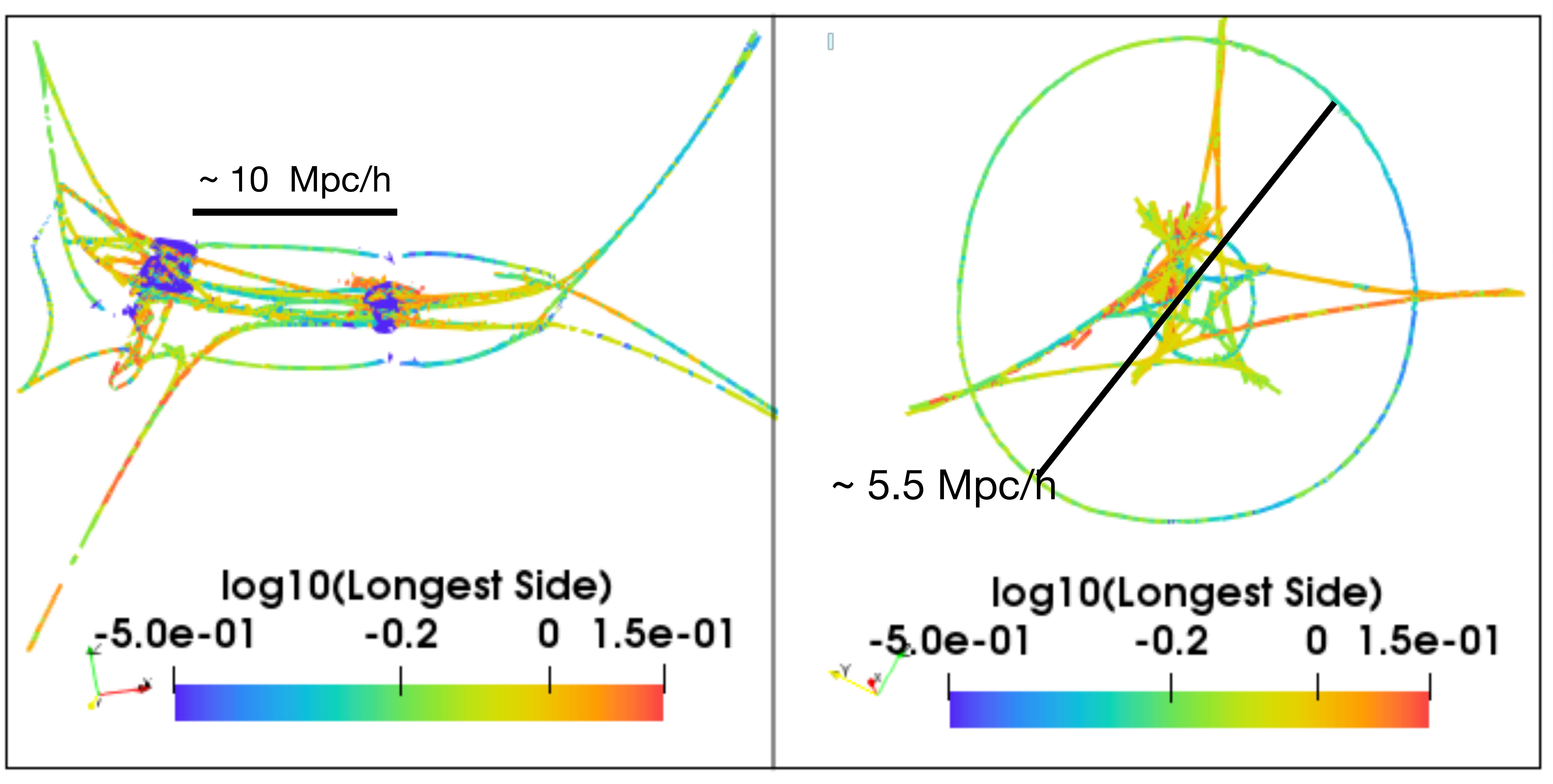

Eulerian space

Lagrangian space

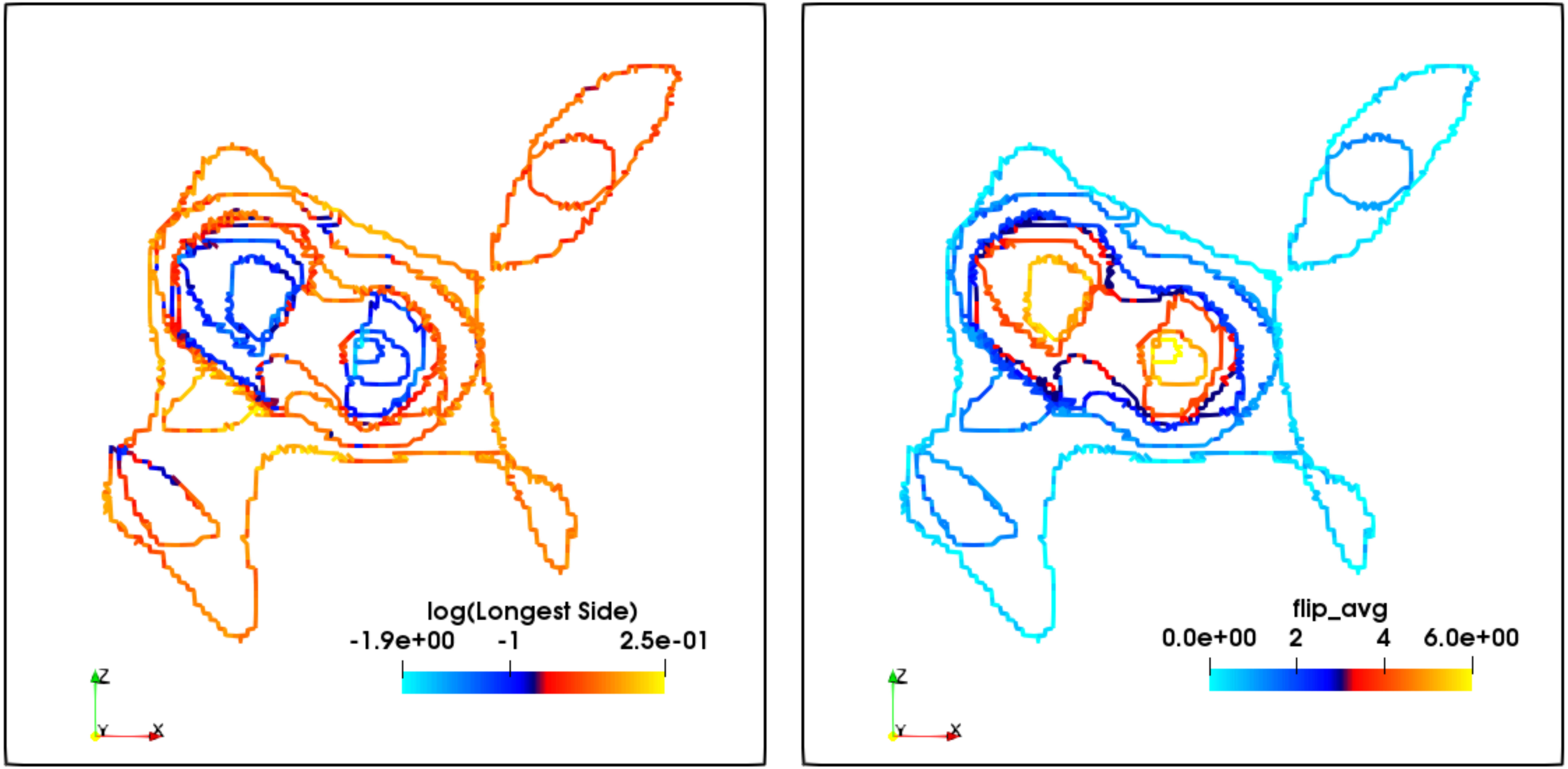

Caustics within a sphere of R ~ 25 Mpc/h

Velocities
(Colors show speed)

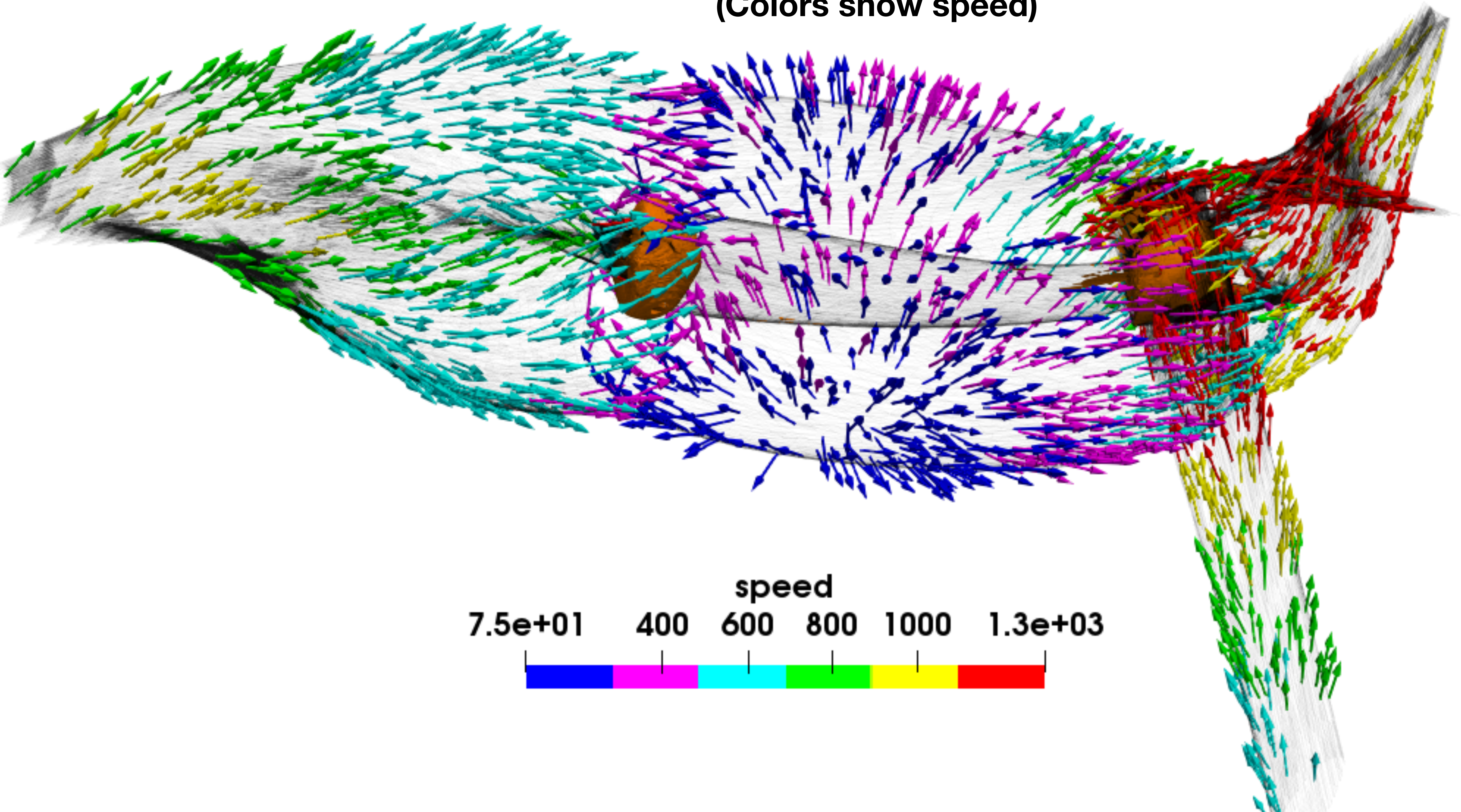

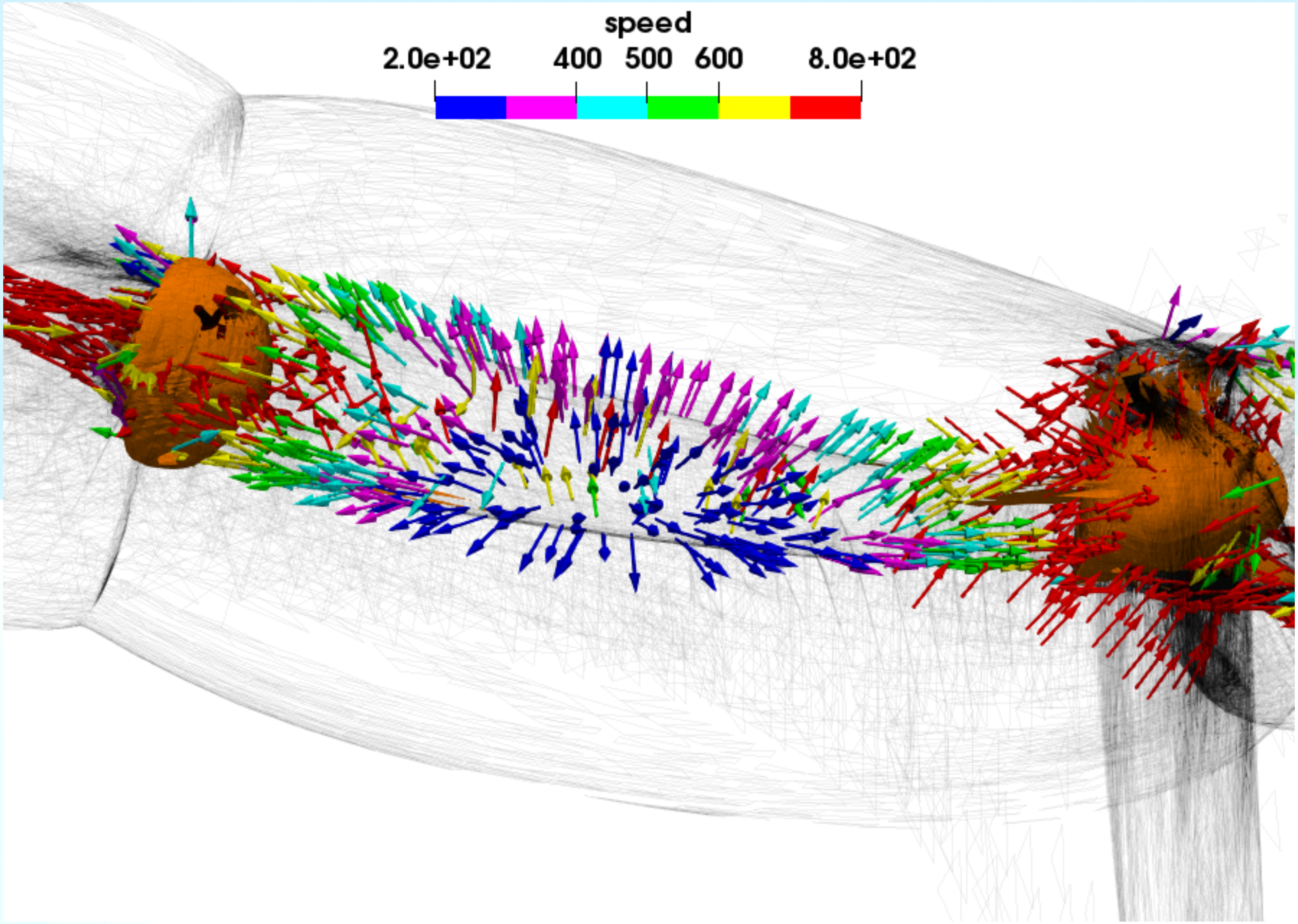
speed
2.0e+02
400
500
600
8.0e+02

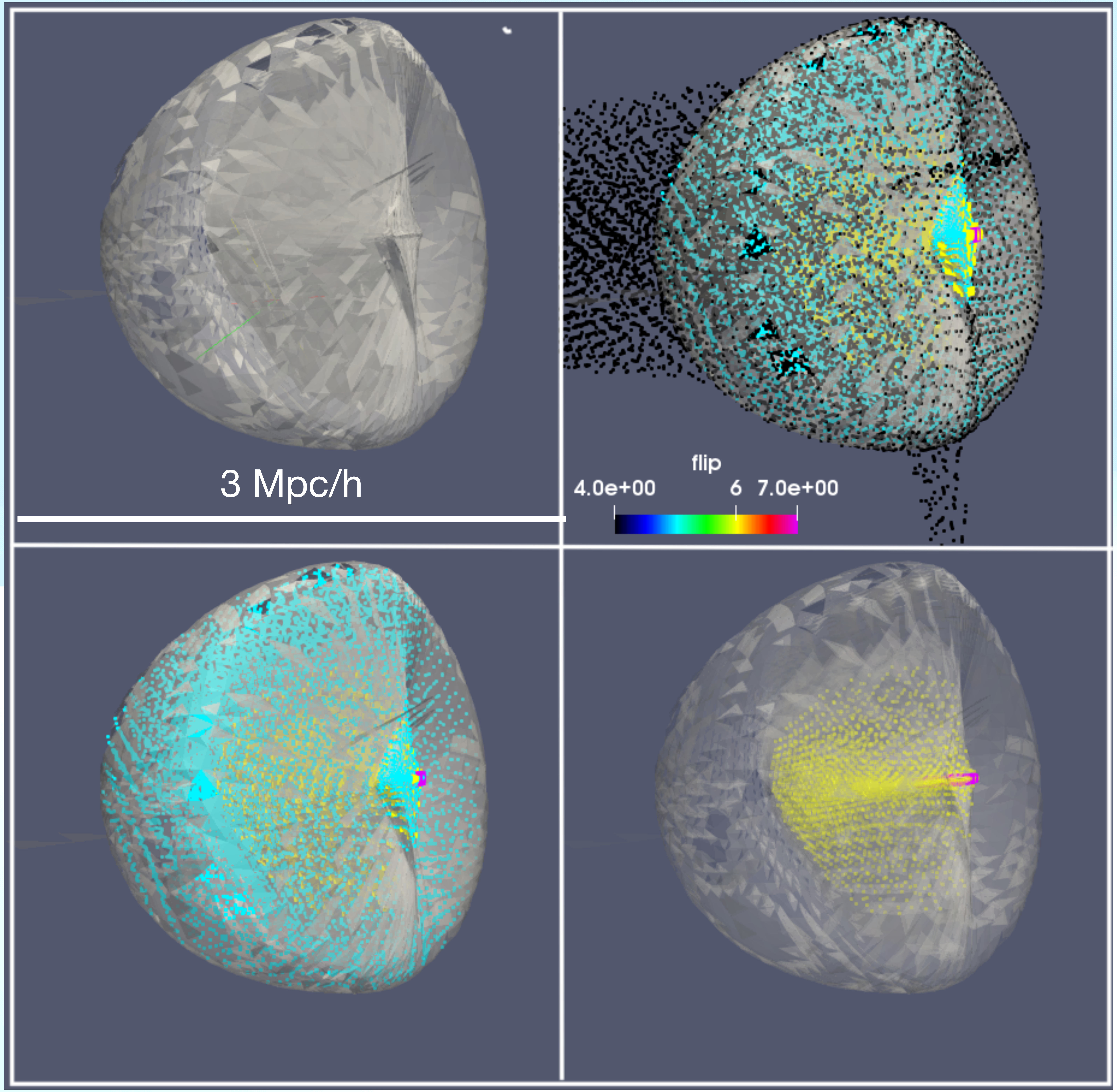

4 <= particles with flip-flops <= 7

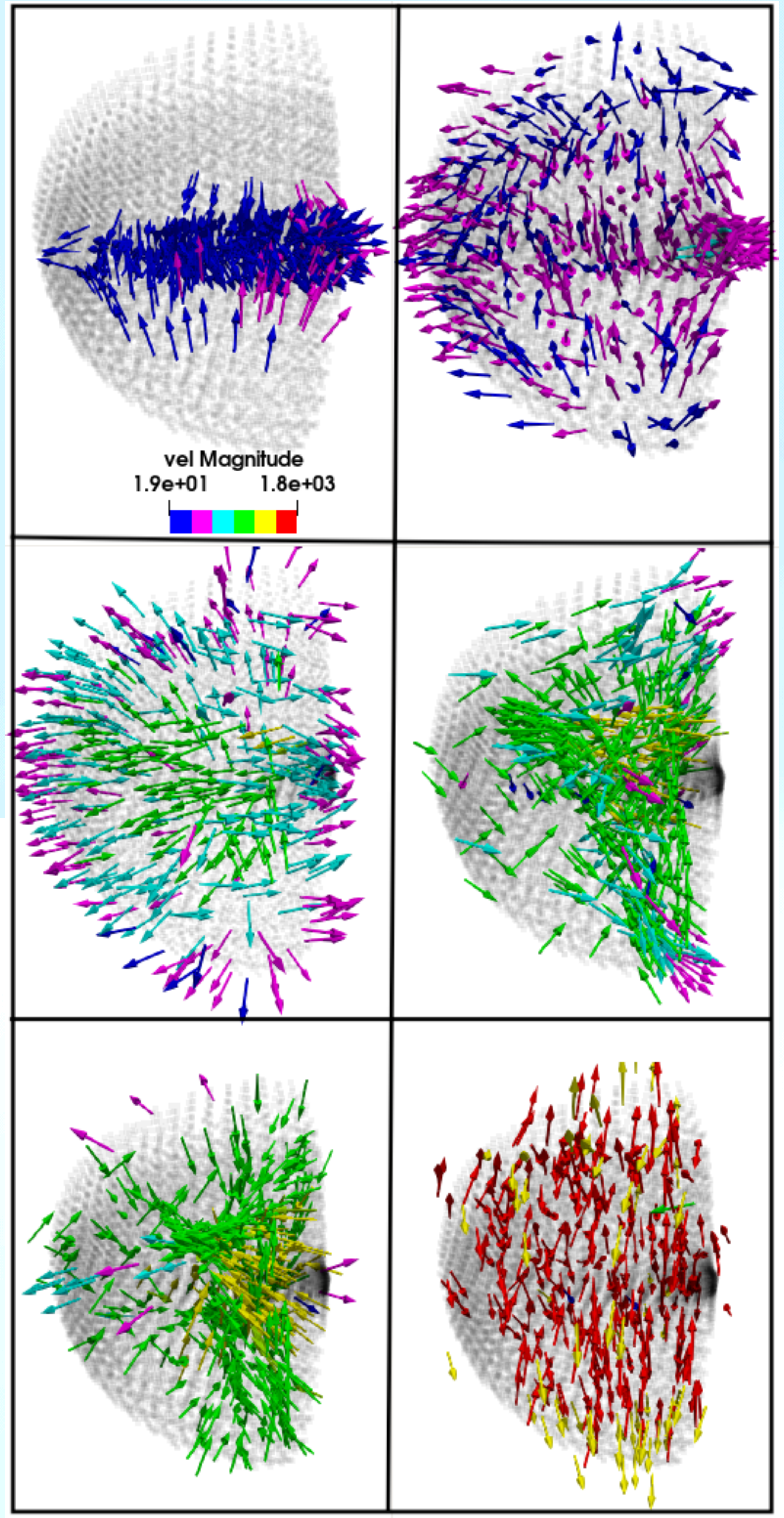

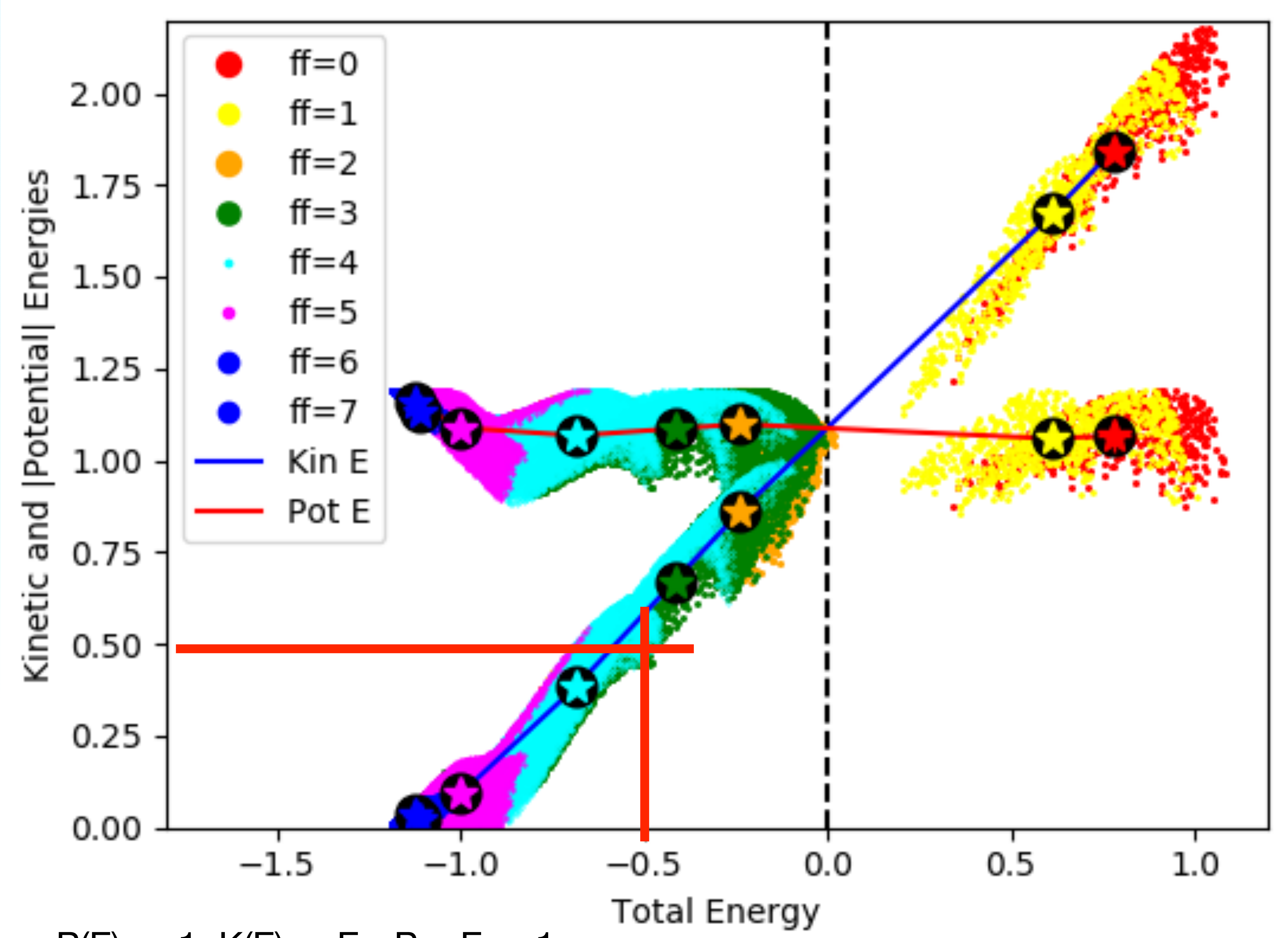

P(E) ~ -1; K(E) = E - P = E + 1

Vir: K = -E; K = -P/2 = 1/2

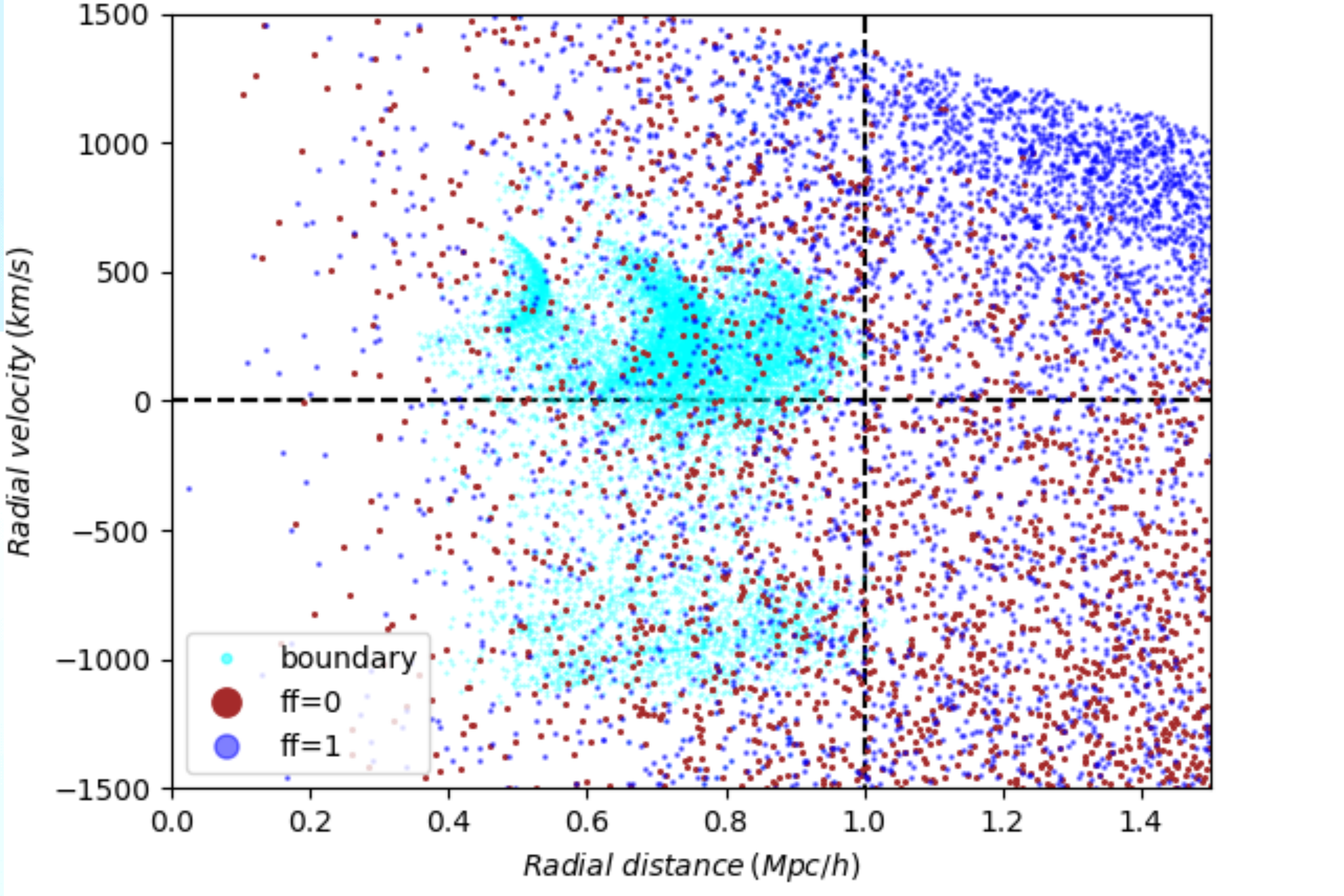
1500
1000
500
0
−500
−1000
−1500
0.0
0.2
0.4
0.6
0.8
1.0
1.2
1.4
Radial velocity (km/s)
Radial distance (Mpc/h)
boundary
ff=0
ff=1

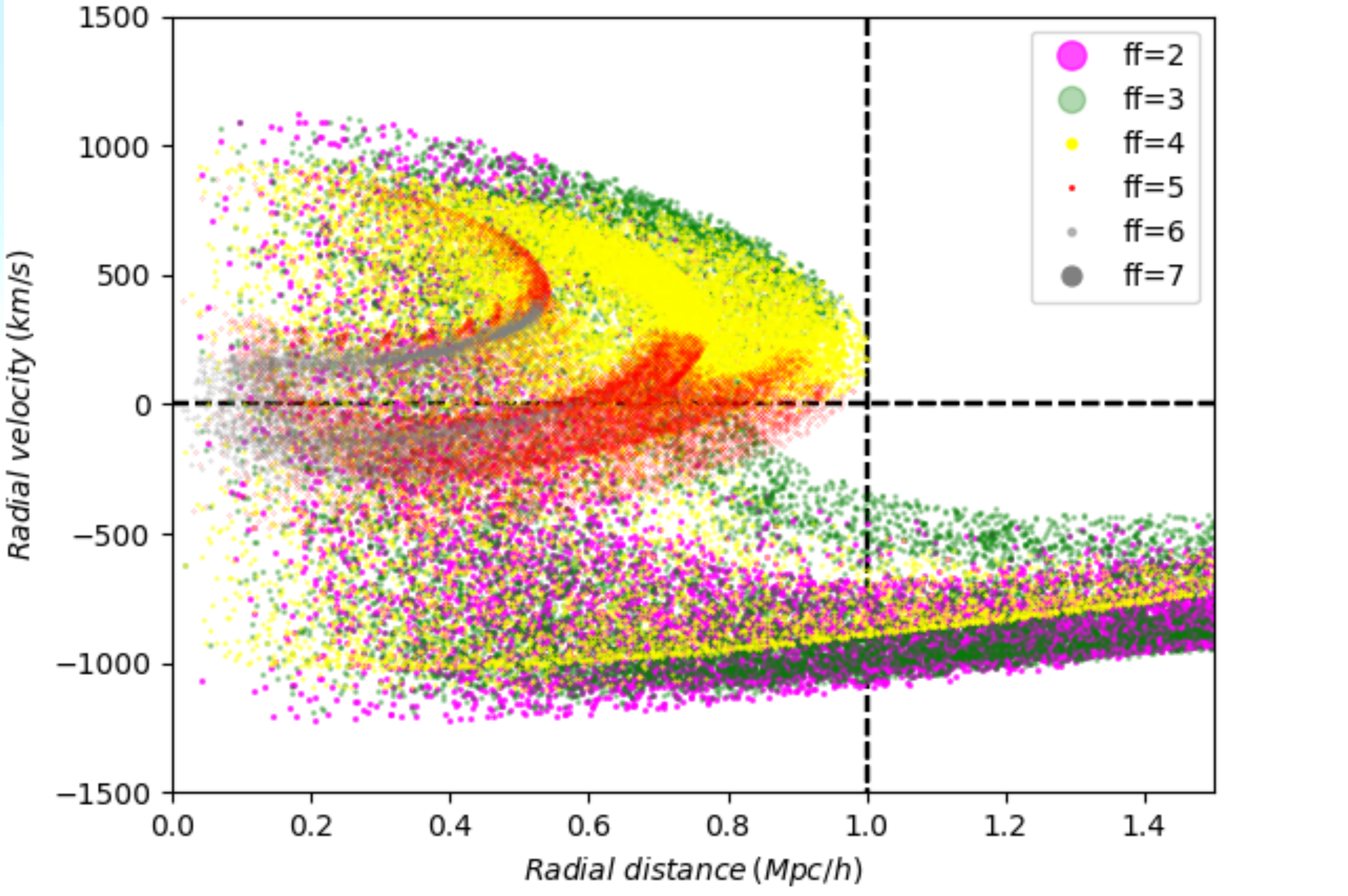
1500
1000
500
0
−500
−1000
−1500
0.0
0.2
0.4
0.6
0.8
1.0
1.2
1.4
Radial velocity (km/s)
Radial distance (Mpc/h)
ff=2
ff=3
ff=4
ff=5
ff=6
ff=7

Shape of the caustic boundary of the halo in E

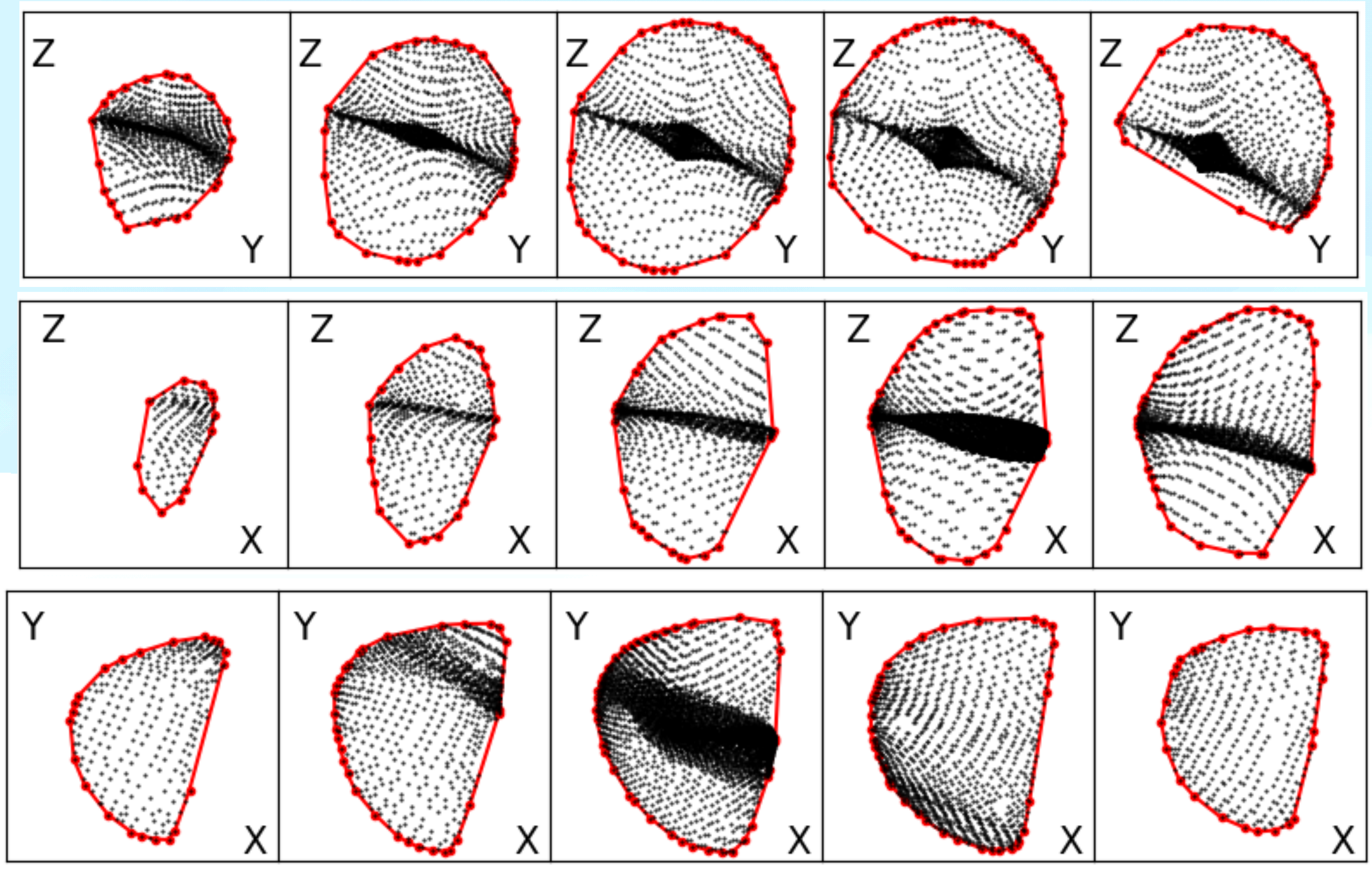

5 slices parallel to
X, Y and Z axes

Black dots are particles
with n_ff > 4

Slice thickness ~ 0.1Mpc/h

Red contours
are 2D convex hulls

Shape of the caustic boundary of the halo in L

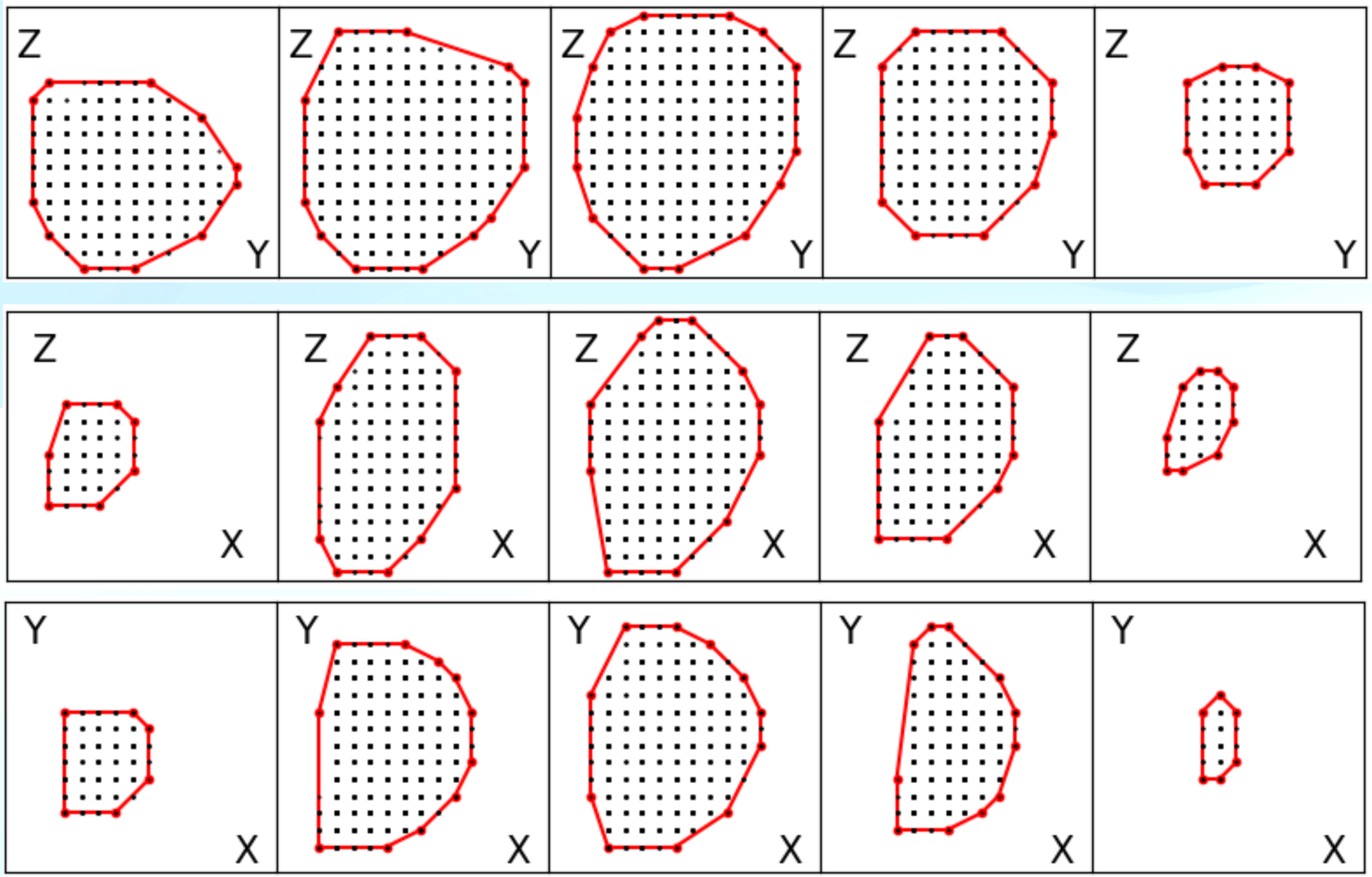

Slice thickness ~0.4 Mpc/h

Three mutually orthogonal slices thought Delaunay tessellations of the both hallos in the dumbbell

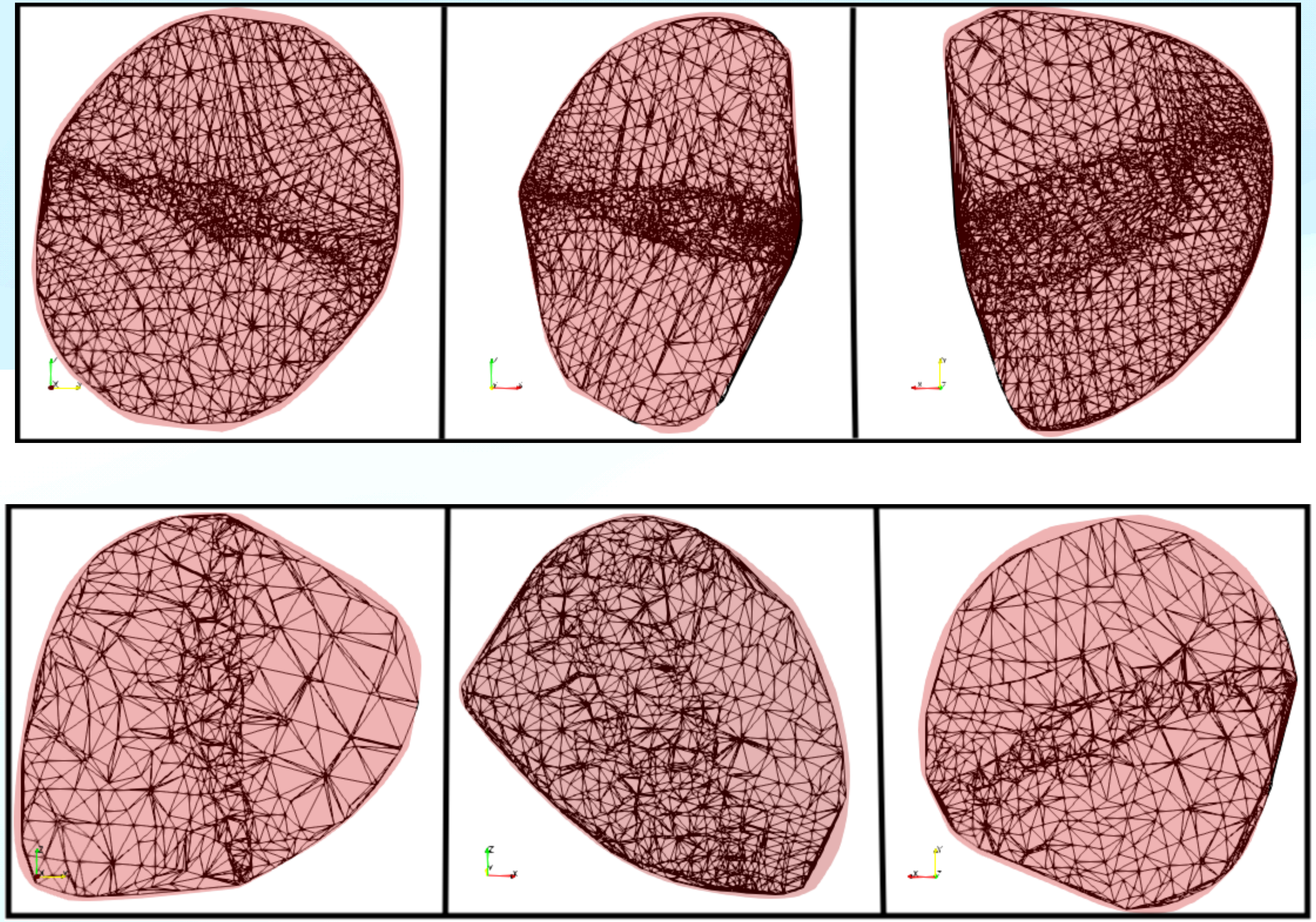

Summary

(*) Caustics allow to study the shapes of the DM web in cosmological simulations without assumptions about their boundaries.

(*) Caustics are not fancy constructions. They are physical objects.

(*) The shapes of caustic are direct products to the complex gravitational dynamics in collisionless media.

(*) The dumbbell structure consisting of two halos connected by a filament is one of the most common structures occurring in N-body simulations.

(*) It demonstrates two cylindrical caustic shells. The radius of the internal shell has the diameter similar to the sizes of the halos attached on both sides.

(*) Both caustic tubes supply mass to the halos.

(*)The halos are neither spherical no ellipsoidal.
However, there shapes look like convex hulles.

(*) The count of flip-flops provide additional indicator helping to sort out multistrim Flows.

(*) There are streems that are not gravitationally bound to halos